Lipid Microfluidic Biomimetic Models for Drug Screening: a comprehensive review

Eduarda Fernandes, Vanessa F. Cardoso*, Senentxu Lanceros-Méndez and Marlene Lúcio*

E.F.*
CF-UM-UP, Centro de Física das Universidades do Minho e Porto and LaPMET – Laboratory of Physics for Materials and Emergent Technologies, Universidade do Minho, 4710-057, Portugal
eduardabfer@gmail.com

V.F.C.*
CMEMS-UMinho, Universidade do Minho, Campus de Azurém, 4800-058, Portugal
LABBELS-Associate Laboratory in Biotechnology and Bioengineering and Microelectromechanical Systems, Universidade do Minho, Braga/Guimarães, Portugal
vcardoso@cmems.uminho.pt

S.L.M.
CF-UM-UP, Centro de Física das Universidades do Minho e Porto and LaPMET – Laboratory of Physics for Materials and Emergent Technologies, Universidade do Minho, 4710-057, Portugal
BCMaterials, Basque Center for Materials, Applications and Nanostructures, UPV/EHU Science Park, 48940, Spain
IKERBASQUE, Basque Foundation for Science, 48009, Spain

M.L.
CF-UM-UP, Centro de Física das Universidades do Minho e Porto; LaPMET – Laboratory of Physics for Materials and Emergent Technologies; and CBMA, Centro de Biologia Molecular e Celular, Universidade do Minho, 4710-057, Portugal

Keywords: lipid biomimetic models, microfluidics, high-throughput screening, in vitro tools

Abstract

Developing new drugs is a complex, time consuming and expensive process, being essential to identify potential pharmacokinetic issues in early stages to avoid investment on non-promising candidates. Nearly half of all drug targets and key drug-metabolizing enzymes are found in intracellular environment, compartmentalized by semipermeable barriers, the cell membranes. Inspired by their lipidic bilayer structure, lipid-based biomimetic platforms are being developed to understand the biochemical and biophysical processes at cellular membrane level. Considering the pharmaceutical industry demands for efficient *in vitro* high throughput screening (HTS) tools, microfluidic technology emerges as a promising solution to address challenges in lipid biomimetic models for screening applications. This involves the transformation of commonly used lipid-based biomimetic models, like supported lipid bilayers and lipid vesicles, to a miniaturized approach and their evolution into a new generation of bilayer models. These include pore-suspended and free-standing lipid bilayers, black lipid membranes, and droplet interface bilayers. This review provides an overview of both generation of lipid biomimetic models used in drug-membrane screening applications. Moreover, it delves into the intricacies of their production through microfluidic approaches and examines their screening applications in drug-membrane interaction. The review concludes with a critical analysis of potential future directions in this rapidly evolving field.

1. Introduction

Drug discovery involves multiple steps from target identification to candidate selection. To ensure the success of potential drugs, thorough testing and optimization, particularly in terms of absorption, distribution, metabolism, excretion, and toxicity (ADMET) profiling, are crucial.[1] Early ADMET profiling has gained significance to avoid pitfall encountered in later stages of drug development,[1b, 2] since the case of fluconazole.[3] The fluconazole case changed the pharmaceutical industry paradigm by reaching the success through a series of structural modifications and optimizations guided by the ADMET profiling feedback. Since then, pharmaceutical industry begun to continuous search for new screening solutions for early *in vitro* ADMET profiling, rather than allowing the pharmacokinetic behavior of drugs to be evaluated *in vivo* and only at later stages of drug development.[4]

Most of drugs and therapeutic agents target either membrane constituents or intracellular parts, and cell membranes as an important physiological barrier can impose restrictions to its efficacy.[5] Drug-membrane interactions are inherent, which can lead to structural and

functional changes at cell membranes; or/and go through structural changes on drug molecules.[5d] Therefore, a comprehensive understanding of these reciprocal interactions on the drug molecule pathway to the target becomes paramount in a rational design and optimization of new drug candidates.[5-6] Notwithstanding, while drug-membrane interactions studies are a settled part of the drug discovery process, it is also increasingly recognized that *in vitro* cell experimental settings have limitations in comprehensively addressing these interactions. Cellular models do not allow to perform controlled biophysical studies or extract information at the molecular level, which is essential for ADMET profiling and molecular optimization.[7] To address these difficulties, lipid biomimetic models mimicking the lipid matrix of cell membranes had emerged as simple yet relevant tools for studying drug-membrane interactions.[5b, 6a, 8] They offer a platform to perform biophysical studies under controlled and adjustable conditions, and their simplicity allows for straightforward characterization of interaction and processes at the molecular level, which is not possible using complex living cells.[6a, 8a, 9] Therefore, these models are important tools for assessing the impact of these interactions on ADMET properties, membrane permeability, and drug-induced membrane toxicity, with reliable information to support drug discovery. Several reviews have been published in this context.[5b, 5d, 6a, 8a, 8b, 9a, 9b]

The demand for adequate models mimicking membrane barriers, also requires the development of screening protocols that provide reproducibility, standardization, throughput, and sustainability to support the drug discovery process. Several efforts have been carried out to standardize the drug discovery process using lipid biomimetic systems with high-throughput screening (HTS) methods in multiple well plates.[10] However, while these HTS methods have been valuable to decrease the attrition rate of pharmaceuticals industries, they present limitations in processing time and requires costly equipment.[1, 11]

Microfluidics has emerged as a promising technology in the seek for new *in vitro* tools to mimic physiological environments for different purposes, presenting cost-effective platforms with improved reproducibility and throughput.[1a, 7b, 12] Their potentialities have led to the miniaturization of thousands of assays performed daily in pharmaceutical and biotechnology laboratories.[12d, 13] The development of biomimetic environments and the use of laminar flow properties in microfluidic channel networks present intriguing opportunities for drug discovery and biophysical research in particular. These advancements have enabled the reliable, scalable, and miniaturized study and characterization of molecular interaction with artificial cell membranes.[14]

The present review reports on the fabrication processes employed to produce lipid biomimetic models and explore the experiments showcasing their potential as HTS tools. Available reviews in literature often cover the formation of lipid bilayers through microfluidic approaches, but they tend to focus on a specific lipid architecture.[15] In contrast, other published works review the application of microfluidics for drug discovery support, more focused on cell-based solutions.[1a, 7b, 11-12, 12e, 12f, 16] The present review, on the other hand, will provide a brief overview of biomimetic lipid-based drug screening models before presenting in great detail their production through microfluidic approaches, and how they are being employed to screen for drug-membrane interaction. The review will conclude with a critical analysis of potential future directions.

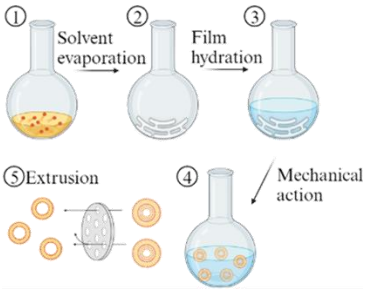
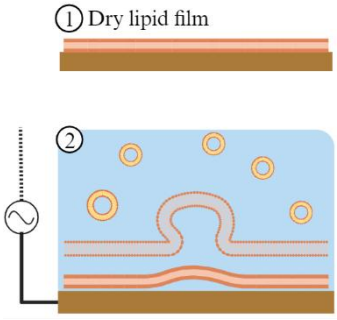
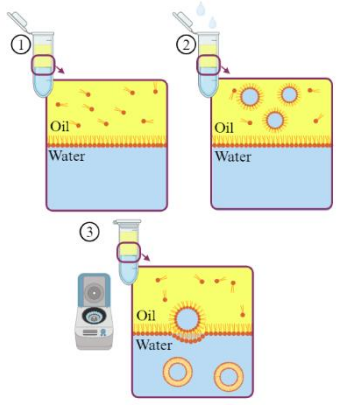
2. Lipid-based models for drug screening

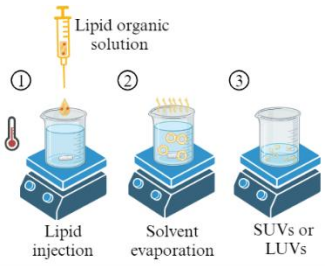
Developing new drugs is a complex, time consuming and expensive process, making it essential to identify potential pharmacokinetic issues in early stages to avoid investing in non-promising candidates.[1b] The rational drug design, in which the chemical structure is modulated based on its pharmacokinetic profile, could constitute a neat strategy to reduce the attrition rate of the pharmaceutical industry.[1b, 17] Current solutions for pharmacokinetic profiling rely on *in vitro* models using living cells and *in vivo* animal studies. However, these models are difficult to conduct, require specific infrastructures and technical expertise, present low reproducibility, are expensive and time consuming. These limitations at such an early stage of drug discovery demand for new strategies for testing libraries of drug candidates in a quicker, reproducible, and more accurate manner. Additionally, regarding a drug rational design, these systems fail on supporting structure-related modifications decisions, since they do not provide an understanding of drug-membrane interactions at molecular level.
Bioinspired systems can be designed to decipher the drug-membrane interactions under controlled conditions.[18] Drawing inspiration from the lipidic arrangement in natural cell membrane, biomimetic systems mimic fundamental structural properties in a simplified manner.[9a] Lipid-based models enable the control of physical and chemical parameters, with particular interest for systematic characterization of drug-membrane interactions, providing insights into the influence of drug candidate physicochemical properties on cell membrane structures.[6b, 18]

Among biomimetic systems, lipid vesicles and supported lipid bilayers (SLBs) are the most widely used.[8b, 19] **Lipid vesicles** can be categorized accordingly its lamellarity and size into multilamellar lipids vesicles (MLVs); and small-, large- or giant unilamellar vesicles (SUVs,

LUVs or GUVs, respectively).[20] Lipid vesicles are highly regarded models due to their physical characteristics and find common use in studying diverse aspects of drug effects on membrane behavior and cell processes.[6a, 9a, 15a, 20-21] They are particularly suitable for investigating drug permeability, involving the determination of partition coefficient, exploration of transport mechanisms, and assessment of membrane toxicity.[9d, 15e, 22] Several conventional methods for producing lipid vesicles have been reviewed,[15e, 22h-j, 23] and the most used ones are briefly described and schematized in Table 1.

Table 1. Brief description of the most widely used methods to produce lipid vesicles.[15a, 23-24] All the schematic representations were created and licensed by BioRender.com.

Formation Method	Brief Description	Advantages (Adv.) and Disadvantages (Dis.)	Schematic Representation
Lipid-film hydration	A lipid organic solution is dried under nitrogen flow or using an evaporator rotator (1). The resultant thin film (2) is then hydrated (3), and through mechanical action, MLVs are formed (4). SUVs/LUVs are obtained through further extrusion through PC filters (5). Sonication can also be used to obtain SUVs.	**Adv.** Straightforward method. **Dis.** Composition and osmolarity can be obstacles; homogeneity dependent on extrusion; and sonication may not ensure homogeneity; small-scale production.	
Electroformation	Lipids organic solution is spread on the electrode surface. The solvent is then removed through vacuum desiccation, forming a dry lipid film (1). The coated electrode is submerged in an aqueous solution, and through application of an AC electrical field, lipids are peeled off and form GUVs spontaneously (2).	**Adv.** Straightforward method to produce GUVs. **Dis.** Results in polydisperse vesicles; challenging to produce GUVs under physiological conditions or using charged lipids.	
Double emulsion	A lipid solution is layered on top of an aqueous solution phase, resulting in a lipid monolayer at the interface (1). The introduction of small volumes of aqueous phase results in inverted micelle (the inner leaflet of liposome) (2). The outer leaflet of the lipid vesicles is formed when the monolayer is forced to enwrap the inverted micelle through centrifugation (3).	**Adv.** Allows the formation of asymmetric lipid vesicles. **Dis.** Traces of organic solvent can remain as residue.	

Solvent injection	An organic lipid solution is dropped into an aqueous phase above the lipid transition temperature (1). The dilution of the organic in water promoted the self-assembly of lipids, which leads to SUVs or LUVs following solvent evaporation (2 and 3).	**Adv.** Simple, reproducible, and simple scale up. **Dis.** Traces of organic solvent and polydisperse vesicle solution.	

Abbreviations: AC – alternating current; GUVs – giant unilamellar vesicles; LUVs – large unilamellar vesicles; MLVs – multilamellar vesicles; O/W – oil/water; PC – polycarbonate; SUVs – small unilamellar vesicles.

SLBs (**Figure 1A**) represent another widely used lipid-based model system with a bilayer structure similar to the cell membrane. Unlike lipid vesicles, which are spherical and more commonly employed in drug permeability studies, SLBs consist of planar lipid bilayers supported on a solid substrate, and are typically used to investigate drug-induced effects at lipid headgroup level, providing insights into the phase behavior and molecular lateral organization of biological membranes.[6a, 8a, 9a, 20] Various methods can be employed to prepare SLBs, including Langmuir-Blodget technology,[25] fusion of lipid vesicles,[26] and spin-coating (**Table 2**).[27]

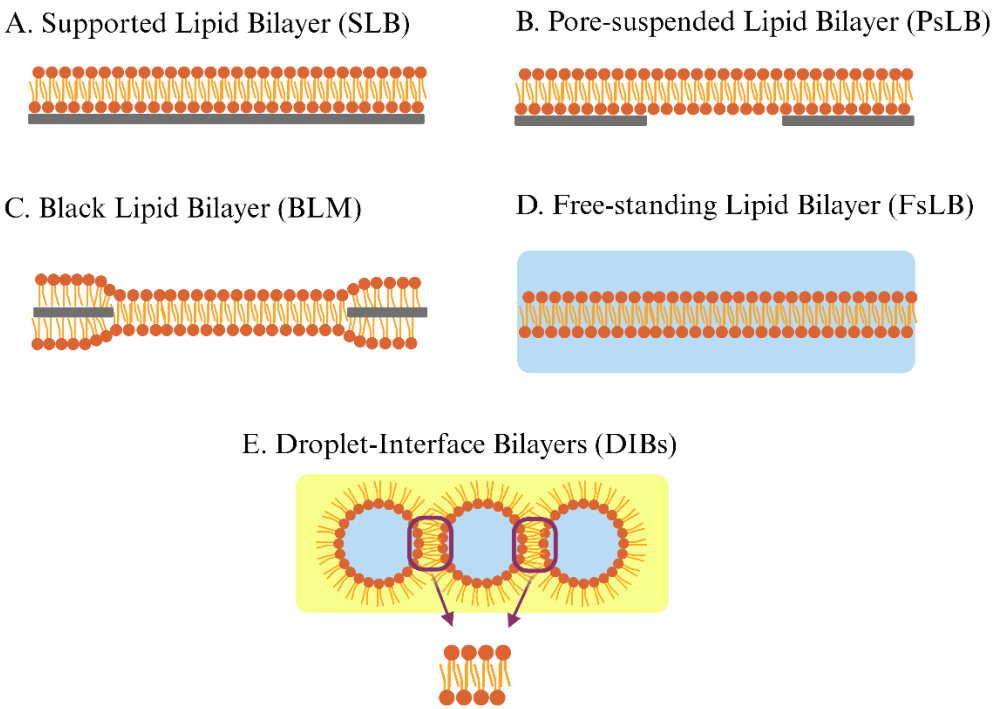
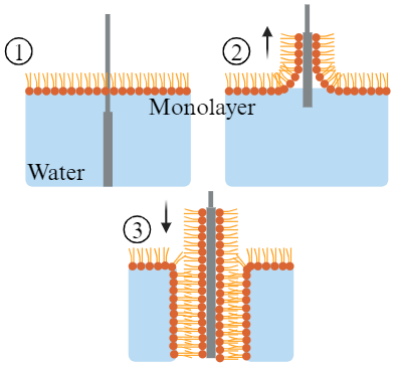
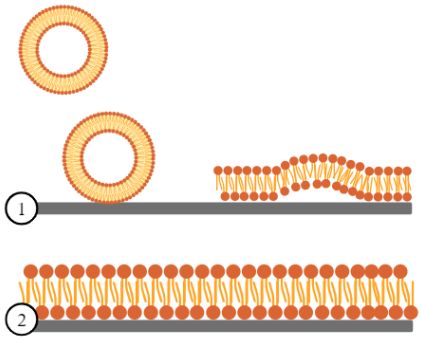
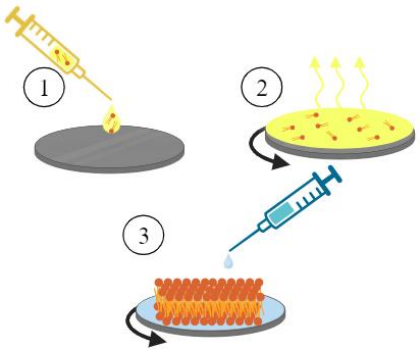


Figure 1. Schematic representation of supported lipid bilayers and its modified-based lipid biomimetic models (not at scale). (Created and licensed by BioRender.com)

Table 2. Brief description of the most widely used methods to produce SLBs.[26b, 27] All the schematic representations were created and licensed by BioRender.com.

Formation Methods	Brief Description	Advantages (Adv.) and Disadvantages (Dis.)	Schematic Representation
Langmuir-Blodgett	A hydrophilic substrate is immersed into an aqueous phase. At the air/water interface, a lipid monolayer is formed and compressed to the required surface pressure (1). Then, the substrate is drawn out of the water perpendicularly to the monolayer, depositing the inner leaflet of the bilayer (2). The substrate is lowered through the monolayer interface to form the outer leaflet layer (3).	**Adv.** Formation of asymmetric bilayer with fewer topological defects, or variations in SLBs. **Dis.** Excludes the use of unsaturated lipids.	
Vesicle Fusion	Involves the spontaneous spreading of SUVs on the substrate surface by exposing it to a vesicle suspension (1). Their instability, triggered by attractive interactions with the clean hydrophilic surface, leads to their disruption and adhesion to the substrate forming a SLBs (2).	**Adv.** Easy, simple, and widely accessible, no sophisticated equipment required. **Dis.** Less reproducible, may exhibit coverage defects and non-fused vesicles. The outcomes are highly dependent on vesicle composition and size, concentration of salts, pH, and temperature.	
Spin Coating	A lipid solution containing a volatile solvent is deposited onto a clean surface substrate (1). After spreading, the substrate is rotated to promote the solvent evaporation, leading to the formation of a thin dried lipid film (2). The substrate is partially or fully hydrated, creating a stack of lipid bilayers (3).	**Adv.** Rapid and straightforward process. **Dis.** Difficult to control the number of layers formed.	

Abbreviations: SLBs – supported lipid bilayers; SUVs – small unilamellar vesicles.

Amidst the growing demand for novel strategies in drug-membrane interaction studies and the evolving adaptation of lipid models to innovative set-ups, several SLBs-derived models have emerged. These include: 1) pore-suspended lipid bilayers (PsLBs), which are described as

SLBs formed in a porous substrate, which are employed for permeability assays and drug-induced biophysical studies (Figure 1B);[28] 2) black lipid membranes (BLMs), comprising a bilayer spanning over a hole, supported only at the extremities and free at the hole center (Figure 1C);[29] 3) free-standing lipid bilayers (FsLBs) formed at the solvent/aqueous interface (Figure 1D);[30] and 4) a more recent approach involving manipulation on a microliter scale, the droplet interface bilayers (DIBs). DIBs consist of droplets where lipids form a monolayer at the oil/water interface, and when two droplets come into contact, a bilayer is formed (Figure 1E).[14, 31]

These SLBs-modified lipid models, PsLBs, FsLBs, BLMs and DIBs, are generally applied for diffusion, permeation and/or transport studies, benefiting from the absence of support (at least in part of the bilayer), which allows the investigation of molecule passage through it. While PsLBs follow similar principles to SLBs, only differing in substrate, FsLBs form at a water/oil interface within microchannels, microcapillaries, or similar structures.[30] BLMs allow the electrical characterization of the transport processes across membranes, and are typically formed using a labor-intensive and time-consuming painting method.[32] This method involves spreading an organic solution of lipids across an aperture of a solid substrate submerged in an aqueous solution. Lipids self-assemble in monolayers at the oil/water interface, and as the bulk organic solvent is removed, the two monolayers meet across the aperture, forming BLMs.[32]

Noteworthy, the several types of lipid bilayers provide overlapping information, but the selection of a specific type dictates the applicable characterization techniques. Each model system described has its own set of advantages and disadvantages. Therefore, the selection of an appropriate membrane model for studying drug-membrane interactions requires an understanding of their inherent properties and careful consideration of the prospected objectives.

3. Biomimetic models produced using microfluidic platforms

In this review, microfluidic platforms will be addressed for applications in: (i) manufacturing methods for biomimetic lipid models; (ii) the study of drug-membrane interactions and drug permeability through membrane bilayers.

The fabrication methods of lipid biomimetic models discussed in this review are summarized in Table 3. Generally, these methods leverage well described batch protocols and adapt them to the microscale. While some methods have proven efficient in producing lipid-based models, not all have been sufficiently adapted to be entirely performed inside a microfluidic

platform. For clarity, in the present review, two types of methods will be distinguished based on the classification "*off microfluidics*" and "*in microfluidics*". A method is classified as "*off microfluidics*" if the final form of lipid biomimetic models is concluded outside the microfluidic set-up; "*in microfluidics*" is used when the model is fully prepared inside the microfluidic device. For instance, in the case of obtaining lipid vesicle arrays, lipid vesicles are previously prepared and then injected into the microfluidic platform to be immobilized over a modified surface, while maintaining the lipid vesicles assembly format (*off microfluidics*). On the other hand, to obtain SLBs by vesicle fusion, SUVs previously prepared are injected into microchannels, and a SLBs is formed over the modified surface, occurring a modification of the lipid system from vesicle assembly format to SLBs (*in microfluidics*). Therefore, in this section both *off microfluidics* and *in microfluidics* approaches are summarized and discussed.

Table 3. Summary of fabrication methods to obtain lipid biomimetic models using microfluidic platforms.

	Lipid System	Fabrication Method	Device Material	Main Observations	Ref.
Off microfluidics	Lipid vesicles	Phase transfer	PDMS	▪ Polydisperse size distribution; ▪ Fabrication of asymmetric GUVs.	[33]
Off microfluidics	Lipid vesicles	Electroformation	ITO or Si	▪ In ITO substrate, less polydisperse distribution; ▪ Lamellar organization dependent on substrate: MLVs on Si and GUVs on ITO.	[34]
Off microfluidics	Lipid vesicles	Arraying	Si oxide	▪ High reproducibility; ▪ Successful immobilization of single and intact GUVs.	[35]
Off microfluidics	Lipid vesicles	Arraying	Glass	▪ Selective deposition of single and intact LUVs; ▪ High LUVs density; ▪ Positioning with 100 nm-precision.	[36]
Off microfluidics	SLBs	Spin-coating	Si	▪ *In situ* characterization; ▪ SLBs stable at least 48 h.	[37]
Off microfluidics	PsLBs	Langmuir-Blodgett and Vesicle Fusion	PDMS	▪ PsLBs stable at least 24 h; ▪ Allows to exchange solutions with microcavities.	[7a]
In microfluidics	Lipid vesicles	Phase transfer	PDMS and glass	▪ Monodisperse size distribution;	[38]

				▪ GUVs diameter linearly correlated to droplet diameter.	
In microfluidics	Lipid vesicles	Phase transfer	PDMS	▪ Monodisperse size distribution.	[39]
In microfluidics	Lipid vesicles	Phase transfer	PDMS	▪ Monodisperse size distribution of asymmetric and unilamellar liposomes; ▪ Customized composition, size and interfacial properties; ▪ Asymmetry as high as 95%.	[40]
In microfluidics	Lipid vesicles	Double emulsion	PDMS	▪ Monodisperse size distribution; ▪ Vesicles with shelf-life for at least 3 months; ▪ Controlled sized (from 20 to 220 μm).	[41]
In microfluidics	Lipid vesicles	Double emulsion	PDMS	▪ Monodisperse size distribution; ▪ Asymmetry lost in 20 and 50% after 1 and 2/3 days, respectively.	[42]
In microfluidics	Lipid vesicles	Double emulsion	PDMS	▪ Monodisperse size distribution of LUVs with tunable diameters.	[43]
In microfluidics	Lipid vesicles	Double emulsion	Glass	▪ Monodisperse size distribution of lipid vesicles-in-vesicles; ▪ Formation of concentric, pericentric and multicompartment liposomes.	[44]
In microfluidics	Lipid vesicles	Octanol-assisted liposome assembly	PDMS	▪ Monodisperse size distribution; ▪ GUVs diameters controlled by flow velocity; ▪ Quick and clean extraction method.	[45]
In microfluidics	Lipid vesicles	Hydrodynamic focusing	Si	▪ Monodisperse size distribution; ▪ Improved throughput on LUVs formation.	[46]
In microfluidics	Lipid vesicles	Double hydrodynamic focusing	PDMS	▪ Improved throughput of cationic lipid vesicles formation; ▪ Smaller particle sizes compared to single hydrodynamic focusing; ▪ Higher unilamellar/multilamellar lipid vesicles ratio.	[47]
In microfluidics	Lipid vesicles	Vertical hydrodynamic focusing	COC	▪ Monodisperse size distribution; ▪ Controlled size from 0.08 to 0.2 μm; ▪ High throughput liposome production (≈ 10^{15} per hour).	[48]

In microfluidics	Lipid vesicles	Microfluidic jetting	Glass	▪ Monodisperse size distribution; ▪ Unconstrained control of content; ▪ High throughput GUVs production (≈ 10^5 per hour).	[49]
In microfluidics	Lipid vesicles	Microfluidic jetting	PMMA	▪ Unilamellar and asymmetric liposomes.	[50]
In microfluidics	Lipid vesicles	Microfluidic jetting	PMMA	▪ Parametric optimization for automatic sequential GUVs generation.	[51]
In microfluidics	Lipid vesicles	Electroformation	Glass	▪ Efficient production of GUVs.	[52]
In microfluidics	SLBs	Vesicle Fusion-based	PDMS	▪ Long-standing SLBs (at least 2 h); ▪ Easier and less expensive surface functionalization; ▪ Heterogeneous microfluidic immunoassay.	[53]
In microfluidics	SLBs	Vesicle Fusion-based	Glass	▪ Efficient method to generate SLBs network; ▪ Dynamic control of in situ composition; ▪ Multiplexing ability.	[54]
In microfluidics	SLBs	SLBs arraying	PDMS	▪ Large-scale parallel bilayer array; ▪ Membrane corrals readily produced in a single step.	[55]
In microfluidics	SLBs	Microcontact printing	Glass	▪ High throughput production of an array using an agarose gel stamp; ▪ Array density of 600 SLBs per cm^2; ▪ Effective transfer of neutral and negatively charged liposomes.	[56]
In microfluidics	SLBs	SALB	Si oxide, Au or graphene	▪ Simple, quick, and efficient protocol; ▪ SLBs formation process takes 1–2 h; ▪ Protocol compatible with different conditions (composition and substrate)	[57]
In microfluidics	SLBs	SALB	Conductive polymers coated by PEDOT:PSS	▪ Better membrane sealing compared to vesicle fusion method.	[58]
In microfluidics	SLBs and PsLBs	Vesicle fusion-based	PDMS	▪ PsLBs stable at least 15 h; ▪ SLBs or PsLBs configuration control depending on bulk pH.	[59]

In microfluidics	BLMs	Painting method	Si/Parylene	▪ Parylene coating suitable for BLMs formation; ▪ Suitable for automated parallel processing.	[29a]
In microfluidics	BLMs	Painting method	PMMA/Parylene	▪ Formation of BLMs on 450 nm diameter micropore; ▪ Bilateral access of both sides of BLMs.	[29b]
In microfluidics	BLMs	Painting method	PMMA/Parylene	▪ Formation of BLMs on 400 nm diameter micropore; ▪ Long-term stability (≈ 120 h).	[29c]
In microfluidics	BLMs	Painting method	PMMA	▪ Simple architecture; ▪ Formation of air-exposed BLMs; ▪ Scalable technique to BLMs array generation.	[29d]
In microfluidics	BLMs	Painting method	PMMA/Parylene	▪ Repetitive formation of BLMs with 8.7 nm thickness; ▪ Simultaneous optical and electrophysiological measurements; ▪ Allow reformation of broken BLMs.	[29e, 32c]
In microfluidics	BLMs	Painting method	PMMA	▪ High reproducibility; ▪ Four BLMs simultaneous formed.	[60]
In microfluidics	BLMs	Painting method	PDMS	▪ BLMs in a microchamber applicable to fluorescence observation and membrane potential modulation.	[61]
In microfluidics	BLMs	Painting method	PDMS/Si nitride	▪ Good sealing BLMs; ▪ High stability (lifetime > 3 h) and high surface yield.	[62]
In microfluidics	BLMs	Solvent exchange	PDMS	▪ Simple device; ▪ High-density BLMs array; ▪ Buffer exchanging without break BLMs.	[63]
In microfluidics	BLMs	DCM	PDMS	▪ Single and double-stacked BLMs with open flow channels at both sides; ▪ Formation with success rate of 50%; ▪ BLMs remained between guide pillars for ≈ 2 h.	[64]
In microfluidics	BLMs	DCM	PEEK/PMMA	▪ Formation of BLMs on 500 nm diameter micropores;	[65]

				▪ Stability requires further improvement.	
In microfluidics	BLMs	DCM	Si/ETFE	▪ Formation of BLMs on 300 nm diameter micropores; ▪ BLMs stable against large voltages.	[32b]
In microfluidics	BLMs	DCM	Aluminum	▪ Single circular BLMs formed with different compositions; ▪ Dynamic control of membrane tension and temperature; ▪ Large area and planar geometry allow fluorescence microscopy; ▪ Lifetime greater than 7 h.	[66]
In microfluidics	BLMs	Hydrostatic pressure	PDMS	▪ Fully automated process; ▪ BLMs formation takes 78 min and presented a success rate of 80%.	[32a]
In microfluidics	FsLBs	Solvent extraction	PDMS	▪ Simple device; ▪ High-quality BLMs	[30]
In microfluidics	FsLBs	Solvent extraction	PDMS	▪ FsLBs formation with a success rate of 100%; ▪ Flat symmetrical and asymmetrical FsLBs, with a lifespan of ≈ 2h.	[67]
In microfluidics	PsLBs	Electroformation	Si/Parylene	▪ Array of solvent-free dome-shaped PsLBs; ▪ Controllable thickness through varying initial lipid concentration; ▪ Allow exchanging of solutions through the aperture.	[28a]
In microfluidics	PsLBs	Vesicle Fusion-based	PDMS	▪ Formation of solvent-free PsLBs; ▪ Sealing resistance dependent on surface treatment; ▪ Easy bilateral access.	[28b]
In microfluidics	PsLBs	Vesicle Fusion-based	Not described	▪ Hybrid membrane formation takes 8.5 h; ▪ Formation of PsLBs with a success rate of 80%; ▪ Membrane stability at tangential flow and osmotic gradient controlled through varying incubation time.	[28c]
In microfluidics	DIBs	Droplet generation	PTFE	▪ Successful DIBs formation with a 3D architecture.	[31a]

In microfluidics	DIBs	Droplet generation	PDMS	▪ High throughput formation and reliable storage of DIBs array.	[14]
In microfluidics	DIBs	Droplet generation	PDMS	▪ High throughput generation of DIBs; ▪ Full control on droplets number and content.	[31b]
In microfluidics	DIBs	Droplet generation	PDMS	▪ BLMs with controllable size and shape; ▪ No cross contamination.	[15d]
In microfluidics	DIBs	Droplet generation	PMMA	▪ Successful pore formation on BLMs; ▪ Exchangeable BLMs.	[68]
In microfluidics	DIBs	Droplet generation	PDMS	▪ Formation of asymmetric DIBs; ▪ Simultaneous electrical measurements on multiple DIBs.	[69]
In microfluidics	DIBs	Droplet generation	PMMA	▪ Automated formation of asymmetric BLMs by controlling rotation frequency; ▪ BLMs ruptures at 140-180 rpm.	[70]
In microfluidics	DIBs	Droplet generation	PDMS and glass	▪ Formation of a honeycomb pattern of DIBs-bounded droplets in a single step.	[71]
In microfluidics	DIBs	Droplet generation	Polycarbonate	▪ Easy and rapid generation of DIBs pairs with controlled compositions; ▪ Array of 12 DIBs in less than 5 minutes.	[72]

Abbreviations: Au – gold; BLMs – black lipid membrane; COC – cyclic olefin copolymer; DCM – droplet contact method; DIBs – droplet interface bilayers; DOPC – dioleyl phosphatidylcholine; DPPC – dipalmitoylphosphatidylcholine; ETFE – ethylene tetrafluoroethylene; FsLBs – free-standing lipid bilayers; GUVs – giant unilamellar vesicles; ITO – indium tin oxide; PDMS – dolydimethylsiloxane; PEDOT:PSS – poly(3,4-ethylenedioxythiophene) polystyrene sulfonate; PEEK – polyether ether ketone; PMMA – poly(methyl methacrylate); PsLBs – pore-suspended lipid bilayers; PTFE – polytetrafluoroethylene; SALB – solvent-assisted lipid bilayer; Si – silicon; SLBs – supported lipid bilayers.

3.1. Formation of lipid-based models *off microfluidics*

3.1.1. Lipid vesicles

Three approaches to lipid vesicles formation *off microfluidics* are discussed in this section: (i) lipid vesicle arrays formed on a surface by immobilization in microwells; (ii) lipid vesicles produced by electroformation, and (iii) emulsion-based methods for producing asymmetric lipid vesicles.

The formation of lipid vesicle arrays requires that unilamellar vesicles are formed outside the microfluidic device by the lipid film hydration method (**Table 1**), and posteriorly injected into the microfluidic platform to be individually immobilized in the microwells.[35-36] To ensure individual vesicle immobilization, the surface of the microwells is functionalized to present sequential repulsive/attractive/repulsive regions, achieved by using two different chemistries: one to prevent adsorption and separate lipid vesicles and the other to anchor them to the surface.[35-36] This double functionalization creates binding regions separated by repulsive regions. The resulting lipid vesicle array can be employed on screening (bio)chemical properties, molecular function or confined chemical reactions over millions of samples. This provides valuable information about the membrane binding of drug candidates or functional responses induced by drug-membrane interaction.[35-36]

Several strategies based on these arrays have been described. Kalyankar *et al*.[35] performed a study in which the surroundings of microfluidic wells were coated using self-assembled monolayer of a PEG oligomer, while the interior of wells were coated with a monolayer functionalized with neutravidin, a biotin binding protein (**Figure 2A**). Thus, lipid biotinylated vesicles were injected into the microfluidic device and were immobilized by binding to neutravidin located at the wells' bottom.[35] In a different study but using the same pair streptavidin-biotin binding strategy, a glass substrate was initially patterned with printed regions of biotinylated bovine serum albumin (BSA) and nonprinted regions with non-biotinylated BSA. Streptavidin is then bound to the printed regions, where vesicles with exposed biotin ligands will selectively be immobilized.[36] Both studies were successful in producing arrays by immobilizing lipid vesicles individually, enabling the use of microfluidics for single-vesicle observation and manipulation.

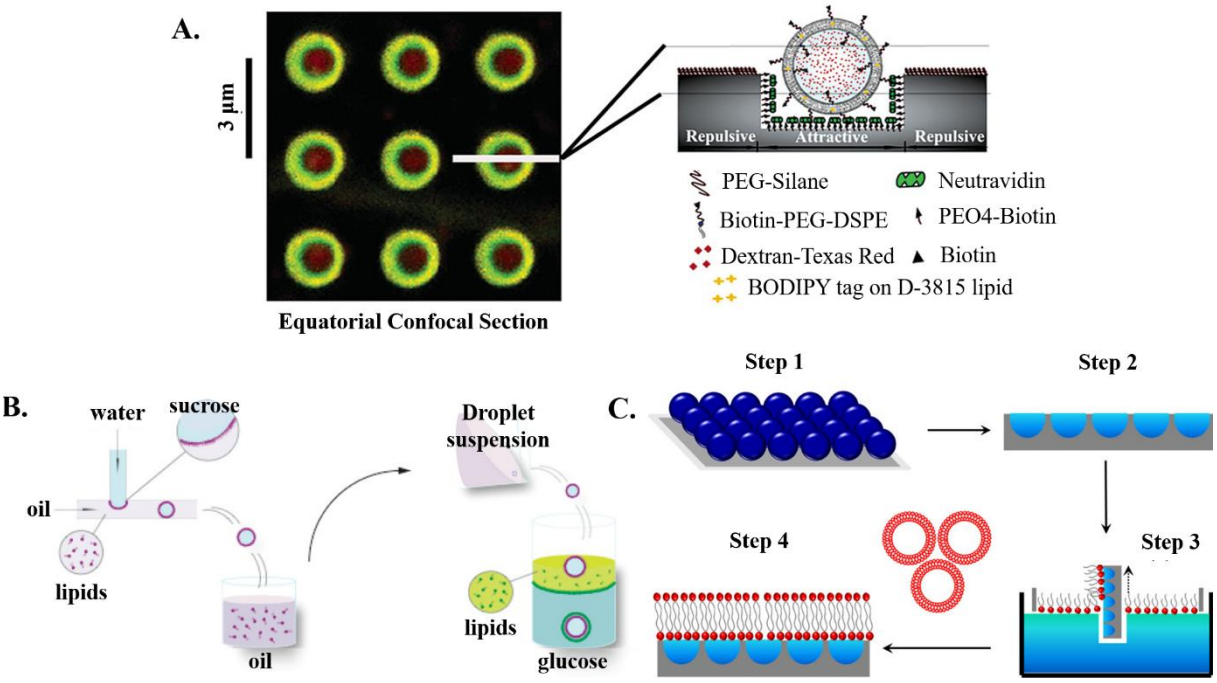


Figure 2. Examples of lipid biomimetic models' formation *off microfluidics*. A) Immobilization of lipid vesicles using the duality of repulsive/attractive surface pattern. Reproduced with permission.[35] Copyright 2006, American Chemical Society. B) An adapted phase transfer process to obtain asymmetric GUVs, in which inner leaflet are formed inside microchannels, but the final stage of outer leaflet assembly is performed *off microfluidics.* Reproduced with permission.[33] Copyright 2011, American Chemical Society. C) PsLBs formation over a substrate by a series of microcavities using a combination of Langmuir-Blodget and vesicle fusion techniques. Reproduced with permission.[7a] Copyright 2019 American Chemical Society.

Another approach to produce lipid vesicles *off microfluidics* by electroformation was conducted by Le Berre *et al*..[34] The main achievements of this electroformation approach included the possibility of controlling the molecular organization of the lipid film by changing the surface properties of Silicon (Si). Four different types of surface treatments were applied to the Si substrates: no treatment, hydrophilized Si, phenyl-modified, and hydrophobized Si. Through surface properties changing, it is possible to control molecular organization and size distribution of the final GUVs, depending on the final application.[34]

The third approach consists of forming asymmetric lipid vesicles through an emulsion-based method (**Figure 2B**). This two-step method begins *in microfluidics* to create the vesicle inner leaflet, followed by an *off microfluidics* step to obtain the outer leaflet.[33] In a T-junction device, aqueous and lipid organic solutions are injected in different inlets. When these immiscible phases come into contact at the T-junction, a droplet of a lipid monolayer enclosing an aqueous phase is formed, corresponding to the inner leaflet. Simultaneously, a monolayer is formed at an aqueous/oil interface in an external vessel for the *off microfluidics* step. The lipid droplets formed *in microfluidics* are collected and dropped into that vessel containing the monolayer and, through centrifugation, the droplets are forced to pass through that interface, forming the outer leaflet of the lipid vesicles.[33] This emulsion-based method allows the formation of asymmetric vesicles, through the tunable constitution of each *in* and *off microfluidics* monolayer. Notwithstanding, this approach does not demonstrate clear advantages over the conventional emulsion-based method.

3.1.2. Supported lipid bilayers

Supported lipid bilayers (SLBs) on a solid support (SiO_2 wafer) were produced *off microfluidics* by spin-coating (**Table 2**), followed by an assemble step of the SiO_2 wafer into a microfluidic cyclic olefin copolymer (COC) chamber.[37, 73] For SLBs production, a lipid mixture dissolved in chloroform is dried and re-dissolved again in isopropanol. The resultant lipid isopropanolic solution is then deposited on the SiO_2 wafer placed on a spin-coater. During the spin-coating process, the rotation of the substrate causes the lipid molecules to spread from the centrally deposited lipid solution. Following the spin-coating process, the substrate is placed in a vacuum chamber to ensure complete isopropanol evaporation. The number of bilayers formed is linearly proportional to the lipid solution concentration.[37] The SLBs-functionalized SiO_2 wafer is then assembled into a COC microfluidic chamber. Microfluid channels are then flushed several times with deionized water to hydrate the SLBs and remove excess lipids.[37] The resulting microfluidic platform containing SLBs allowed for the *in situ* characterization through X-ray reflectivity and fluorescence microscopy.[37, 73]

3.1.3. Pore-suspended lipid bilayers (PsLBs)

In an innovative approach for permeation studies, a combination of vesicle fusion and Langmuir-Blodgett, the most commonly techniques to form SLBs *off microfluidics*, was employed to create PsLBs over a series of microcavities (**Figure 2C**).[7a] The process involves spreading a lipid monolayer at an air/water interface, while microcavities are patterned on a

PDMS substrate using polystyrene beads as mold. The patterned PDMS substrate is dipped onto the air/water interface monolayer, forming the bottom leaflet of the lipid bilayer through Langmuir-Blodgett technique. Subsequently, a lipid vesicle dispersion is dropped over the microcavities, and the vesicles are spontaneously disrupted by the presence of the monolayer, resulting in the formation of PsLBs through the microcavities. A final rinsing step is performed to remove excess lipids and maintain the hydration of the lipid bilayer.[7a]

3.2. Formation of lipid-based models *in microfluidics*

3.2.1. Lipid vesicles

The formation of lipid vesicles *in microfluidics* devices typically employs one of four main approaches: emulsion-based technique, hydrodynamic focusing, microfluidic jetting and electroformation ***(Figure 3)***.

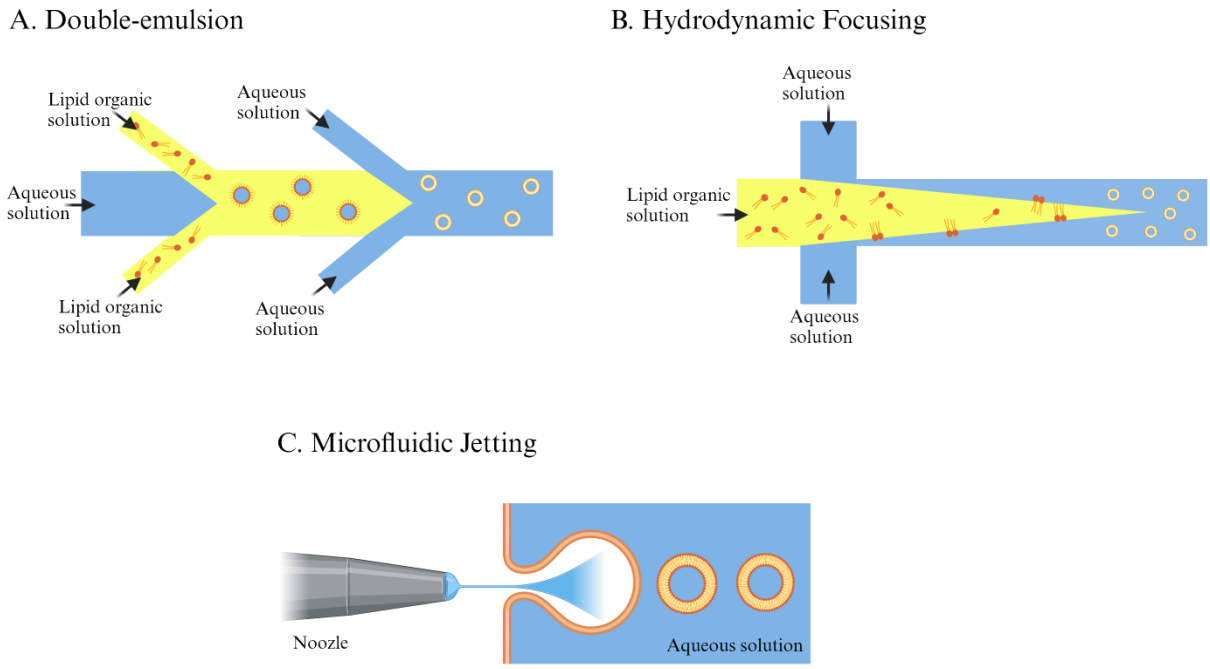


Figure 3. Schematic illustration of different techniques used to form lipid vesicles *in microfluidics*: A) Double-emulsion based; B) Hydrodynamic focusing, and C) Microfluidic jetting. Created and licensed by BioRender.com

Emulsion-based techniques: Concerning the phase transfer methodology, a microfluidic device constructed of PDMS bonded to a glass substrate was fabricated to generate stratified multi-phase flow for controlled synthesis of lipid vesicles.[38-39] In both microfluidic

configurations, water/oil (W/O) droplets are initially formed through flow focusing and then transferred over an oil/water (O/W) interface to promote the self-assembly of the lipid bilayer ***(Figure 3A)***. While Karamdad *et al*. used a step junction for a larger and deeper channel to support the transference,[39] Matosevic *et al*.[38] purposed the microposts to promote it ***(Figure 4A)***.

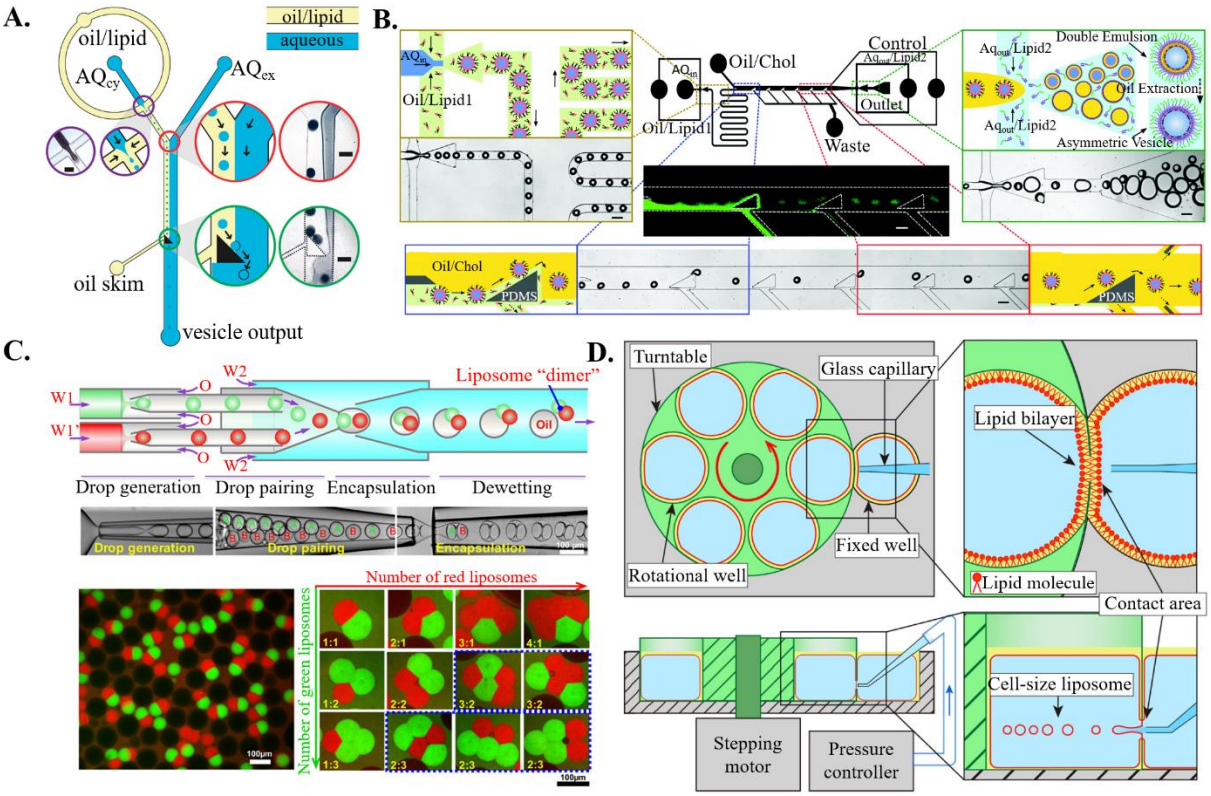


Figure 4. Formation of lipid vesicles *in microfluidics*. A) Circuit schematic and operation of the microfluidic assembly line to generate liposomes in a droplet flow guided by microposts. Reproduced with permission.[38] Copyright 2011, American Chemical Society. B) Schematics of a developed device to generate asymmetric vesicles from W/O/W double emulsions at high-throughput. Reproduced with permission.[42] Copyright 2019, Royal Society of Chemistry. C) Drawing, snapshots and confocal images of fabrication of double emulsions with two distinct drops towards formation of lipid vesicles with distinct multiple compartments. Reproduced with permission.[74] Copyright 2016, American Chemical Society. D) Conceptual scheme of an automatic lipid vesicles generation system on a microfluidic jetting approach. Reproduced with permission.[51] Copyright 2019, Elsevier.

The phase transfer method supported by microposts has been also described to obtain monodisperse asymmetric vesicles.[40] The simultaneous control of their size, lamellarity and

luminal content was accomplished by a triangular post region and two flow focusing regions.[40]

Several microfluidic approaches have been developed based on the double emulsion concept. In contrast to the conventional method (described in **Table 1**) that often produces polydisperse droplets, microfluidic setups enable the generation of monodispersed and size-controlled vesicles through sequential droplet generation.[24d, 24e] The production of double emulsions in microfluidics requires synchronization of the frequency of emulsion droplet formation and specific channel wettability, since oil droplets only can be formed at hydrophilic junction, whereas aqueous droplets only forms at the hydrophobic junction.[24e] The first miniaturization for single-step water/oil/water (W/O/W) emulsion generation was demonstrated using a simple cylindrical microcapillary device with a constriction.[75] Maktabi *et al*. purposed an approach to obtain asymmetric vesicles mimicking the inner and outer leaflets of the Gram negative membranes from asymmetric W/O/W double emulsion ***(Figure 4B)***.[42] To this end, two emulsions (O/W and W/O) with different lipid compositions were combined through a dewetting process of the ultrathin oil shells, yielding asymmetric lipid vesicles.[42] A surfactant-assisted strategy to form vesicles from W/O/W double emulsions was also purposed for the formation of uniform concentric vesicles ***(Figure 4C)***.[44, 74] The T-junction configuration was also employed in a nozzle geometry device comprising two successive T-junctions for the continuous production of stable and monodisperse lipid vesicles.[41] In this flow-focusing setup, at the first T-junction, a W/O emulsion is formed, while the conclusion of the double emulsion occurs at the second T-junction. This involves the contact of the W/O emulsion stream with an aqueous solution, followed by a controlled dewetting process of the oil from the middle layer, ultimately yielding lipid vesicles.[41] Mitigating the lagging oil extraction from the middle layer of W/O/W emulsion, the conventional oil/alkaline lipid solution was replaced by an alcohol-based one. The octanol-assisted liposome assembly (OLA) yielded monodisperse GUVs in a single step process coupled with short vesicle maturation periods, enabling high-throughput production.[45]

Hydrodynamic Focusing: Hydrodynamic focusing involves multiple immiscible liquid streams with specific rates that come into contact (**Figure 3B**). In this method, lipid vesicles formation occurs by introducing a stream of lipids in alcohol through a central channel and constricting the lipid dispersion with two perpendicular/oblique aqueous streams.[76] Typically, the microfluidic configuration is a three-inlet device, where the central stream is focused between two outer streams that flow in a Y shape.[15a] Increased flow rates of the

outer streams compress the width of the central stream.[15a] Jahn *et al*.[46] demonstrated this principle, where a lipid in isopropanol solution flows through the center inlet channel, and an aqueous phosphate-buffered saline solution flows through the two outer inlet channels. Vesicles assembly is energetically favorable at specific points in the system where the alcohol/buffer mixture reached a critical condition and lipid solubility is low.[46] The device length and shear forces from the flux rates determine the liposomes size,[46] and are usually associated with mass production of uniform structures.[15a, 46]

Addressing the low throughput due to the limited volumetric flow rates imposed by planar platforms,[76-77] new ones with a double hydrodynamic flow-focusing region[47] or adopting a vertical flow-focusing geometry were introduced.[48] Comparing a single hydrodynamic focusing and in a double hydrodynamic focusing setup, Balbino *et al*.[47] investigated the impact of multiple parameters, including fluid flow velocity, flow rate ratio, and total lipid concentration, on the formation of cationic liposomes. The authors found that unilamellar vesicles were produced in both, with the double hydrodynamic focusing setup capable of generating smaller particles at high flow rates.[47] Moreover, Hood *et al*.[48] introduced a high aspect ratio microfluidic vertical flow focusing, creating a vertical stack of wide but shallow channels. The high aspect ratio channels enable the lipid stream to be focused in a vertical stack, significantly increasing the throughput for continuous flow assembly of lipid vesicles, while maintaining size control.[48]

Microfluidic jetting: Another method for lipid vesicles assembly involves a pulsed jet flow of an aqueous solution through a preformed planar lipid bilayer between two water droplets (**Figure 3C**). Inspired by the formation of soap bubbles from a soap film, this method allows the assembly of controlled-sized lipid vesicles in large quantities.[15a, 24a, 49] The process includes forming a bilayer by carefully bringing together two lipid-stabilized water droplets and using a micro-nozzle or micro-pipette to eject tiny aqueous solution jets. These jetted volumes wrap in the lipid bilayer, and as they move away from the aperture, the bilayer pinches away, creating a vesicle. Essentially, this approach involves three stages: initial membrane protrusion, membrane collapse and encapsulation, and separation of the vesicle from the bilayer membrane.[49]

Several microfluidic approaches employ this technique. Stachowiak *et al*.[49] initially demonstrated the use of a precisely controlled jet driven by a piezo-actuated syringe to deform a lipid bilayer membrane into a GUV capable of incorporating membrane proteins.[78] Later, the ability to manipulate vesicle size by adjusting the amplitude and number of pulses

during periodic jetting was reported.[49] Furthermore, nano-sized liposomes were obtained by applying long-duration, high-pressure pulsed-jet flows.[50] The main strength of this technique lies in its high-throughput configuration, enabling the formation of thousands of vesicles per minute.[49, 79] Drawback of this technique have been identified. Kirchner *et al*.[80] found through Raman scattering spectroscopy a significant amount of residual organic solvent n-decane, which is a critical component in the process, randomly distributed over the surface area of the lipid vesicles and with variable thickness.[80] Another significant challenge lies on handling difficulties, as the droplets forming the bilayer are created by manual pipetting, and the protocol needs adjustment due to its high dependence on solution properties.[15b, 24c] Addressing the limitations of manual processes, Gotanda *et al.* modified a microfluidic system originally designed for forming DIBs to generate lipi vesicles automatically using the microfluidic jetting technique (**Figure 4D**).[51] The microdevice, featuring six wells on a circular rotation table, was connected to a stepping motor and a dispenser for pulsed-jetting flow, all controlled by a microcomputer. The stepping motor controls rotation speed, rotation duration, and rotation position of the circular turntable, while the dispenser controls the timing of the pulsed-jet flow. In practical terms, as the microcomputer activates the stepping motor at a given rotation, two droplets make contact, and a planar bilayer is created at their interface. The pulse-jet flow is then triggered by a signal from the microcomputer, deforming the planar lipid bilayer into cell-sized vesicles. Through processing both the loop of rotation and the jet application, GUVs are generated in every rotational well automatically.[51]

Electroformation: Kuribayashi *et al*.[52] employed the electroformation technique to produce lipid vesicles *in microfluidics*. Various types of GUVs were assembled inside the channels, which are sandwiched between glass slides coated with transparent indium tin oxide (ITO) electrodes, through an alternating current (AC) voltage.[52] The authors conducted two experiments using the same concept: in the first experiment, they formed lipid vesicles in a single microchannel for characterization, and in the second experiment, they demonstrated the feasibility of preparing GUVs with different lipid compositions in two independent microchannels. An organic lipid solution was deposited on the substrate to form lipid films. After solvent evaporation, facilitated by a nitrogen flow, deionized water was injected into the microchannels, and an AC signal was applied for a few seconds to form GUVs.[52] Despite the method's adaptation for microfluidic setup, the main drawback of the electroformation process persists: its inapplicability to high ionic strength solutions, limiting investigations to conditions less relevant to physiological scenarios.

3.2.2. Supported-lipid bilayers

Although a variety of well-established methods exist for obtaining supported lipid bilayers (SLBs), the microfluidic approaches for forming SLBs *in microfluidics* revolve around the concept of vesicle fusion.

Vesicle fusion-based: Formation of SLBs via vesicle fusion involves the adsorption of lipid vesicles to a substrate, followed by their rupture, fusion and bilayer spreading.[26b] This technique is regarded as simple, versatile, and widely accessible, as it does not require sophisticated equipment.[26b] Although this method is widely used on specific surfaces such as gold, glass and mica, vesicle fusion has also demonstrated potential for forming SLBs on plastic supports.[81] The adaptation of this technique to micrometer-sized systems has been achieved through various approaches.[53, 81-82] SLBs through vesicle fusion were achieved on a plasma-oxidized PDMS substrate, by injecting a lipid vesicle aqueous dispersion into each channel until it filled the outlet syringe wells.[53] In a groundbreaking demonstration, Jönsson *et al*.[82] showed that introducing bulk flow inside the channel provides enough shear force, when high enough, to move the bilayer. Later, the shear forces produced by the bulk flow above the SLBs were used to seal the SiO_2-coated glass floor of the microchannels.[59] In a PDMS cross-shaped device (**Figure 5A**), lipid vesicle dispersion and buffer solution are injected through arm 1 and arm 4, respectively, with arms 2 and 3 remaining opened.[59] The laminar flow prevent any fluid mixing, while confining the vesicles to the left of the channel. In this designated area, vesicles adhere to the SiO_2-coated glass slide, and the subsequent vesicle fusion process leads to the formation of SLBs.[59] Once the excess vesicles are removed, and arms 2 and 3 are closed, the SLBs is efficiently propelled by the shear force to move towards a region encompassing embedded wells.[59] This method demonstrates an intricate interplay of fluid dynamics and surface interactions to precisely engineer SLBs in a microfluidic setup. Remarkably, the behavior of whether SLBs span the well or follow its contours is dictated by the pH of the bulk solution, making this technique adaptable for the formation of PsLBs as well.[59]

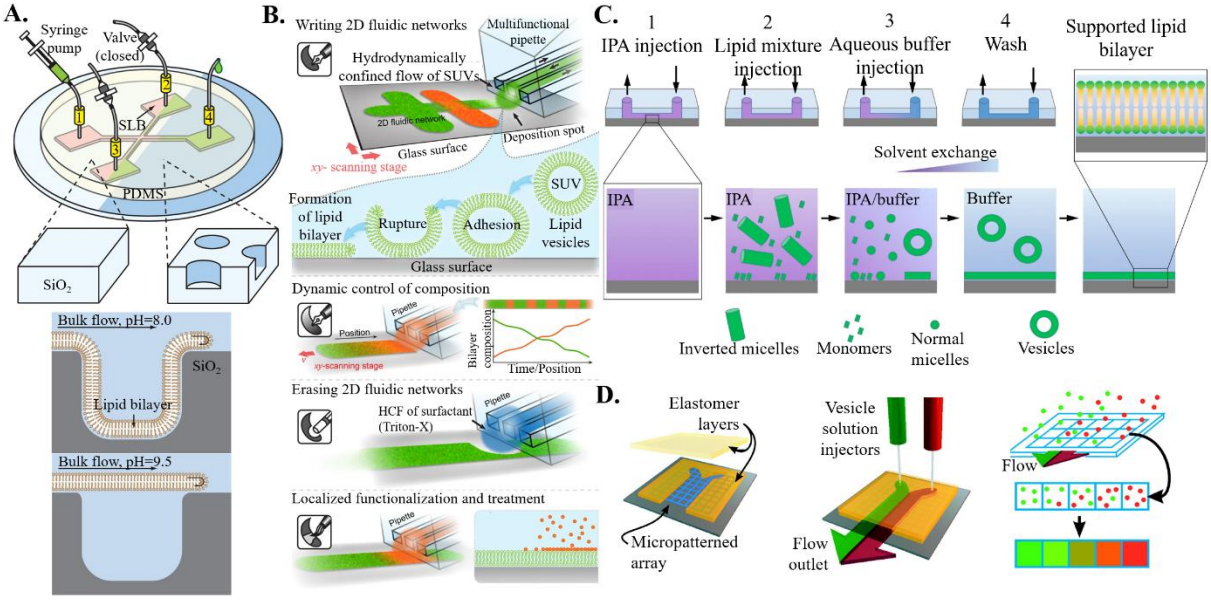


Figure 5. Formation of SLBs *in microfluidics* using vesicle fusion based methods. A) Schematic illustration of the microfluidic device containing four arms used to obtain SLBs in a format dependent on pH of bulk flow. Reproduced with permission.[59] Copyright 2010, American Chemical Society. B) Toolbox based on a multifunctional pipette developed to write/erasing 2D fluidic networks of SLBs by dispensing SUVs to a confined region on a glass substrate. Reproduced with permission under the terms of the CC-BY 3.0 license.[54] Copyright 2013, the Authors. Published by Springer Nature. C) Illustration of the SLBs formation stages by solvent-assisted lipid bilayer (SALB) method. Reproduced with permission.[57] Copyright 2019, Springer Nature. D) Schematic representation of an approach used to obtain parallel array of SLBs with different compositions created by flow and irreversible binding of vesicles to the substrate. Reproduced with permission.[55] Copyright 2000, American Chemical Society.

Ainla *et al.*[54] developed a toolbox to construct 2D nanofluidic networks of SLBs (**Figure 5B**). Employing a multifunctional pipette, they dispensed SUVs dispersion in proximity to a planar surface, inducing vesicle adhesion and subsequently fusion on bilayer formation.[54] The toolbox components include writing, dynamic control of composition, erasing, and local lipid film modifications. Moreover, altering the device position along *xy*-plane enabled the generation of lipid membrane patterns swiftly and flexibly.[54]

As an alternative to typical vesicle fusion method, solvent-assisted lipid bilayer (SALB) was introduced to form SLBs (**Figure 5C**).[57, 83] Basically, a water-miscible organic solvent, like isopropanol, is injected into the microfluidic channels, followed by the injection of a freshly prepared lipid solution in the same organic solvent. At this point, inverted micelles form

inside the microchannels, and upon exchanging the bulk solution with aqueous solution, the lipids self-assemble into normal micelles or vesicles. As the water fraction in the solvent system increases, these lipid structures adhere to the substrate, culminating with vesicle fusion into SLBs formation.[57] The SALB method was successful in forming mixed SLBs comprising a liquid-crystalline phase of DOPC and a gel phase of DPPC inside the microfluidic channels.[84] Additionally, SALB method was employed in a conducting polymer device, showing improved membrane sealing compared to typical vesicle fusion method.[58] Described as simple, requiring minimal sample preparation, and efficient for uniformly spreading SLBs on various material supports, the SALB method is compatible with diverse lipid compositions, substrates and water-miscible solvents.[57, 85]

Other vesicle fusion-based approaches are being introduced for the formation of SLBs arrays. While various techniques, including lithographic methods, microcontact printing, blotting, and polymer lift-off procedures, have been developed for patterning SLBs,[86] they still largely exploit the deposition of lipid vesicles and subsequent vesicle fusion phenomenon.[56, 86] Microcontact printing involves using a stamp, like PDMS[87] or agarose,[56] against a lithographically patterned surface to transfers the lipid material to the solid substrate.[56, 87] Majd *et al*. used hydrogel stamps to form arrays. Each post on the patterned surface was pressed against an agarose stamp with a lipid vesicle suspension. After the posts absorb the lipid dispersion, they were stamped onto the glass substrate.[56] Following stamp removal, the patterned substrate was immersed in deionized water or buffer solution.[56] Lithographic methods can selectively destroy regions of a continuous SLBs to produce patterned lipid bilayer arrays.[86] A parallel bilayer array with defined variation in SLBs composition was developed, in which a prepatterned PDMS surface is exposed to a gradient vesicle flow with different compositions (**Figure 5D**).[55] The vesicles are irreversibly captured on the coverslip, and subsequently continuous SLBs are formed through vesicle fusion phenomenon. The patterned surface define regions with different lipid compositions for each corral.[55]

3.2.3. Black lipid membranes

Black lipid membranes (BLMs) were introduced by Muller *et al*., who spanned a lipid bilayer over a hole approximately 200 μm in diameter using the painting method of an organic lipid solution.[88] Although painting method is described as simple, two drawbacks can be identified: residual solvent and a relatively short lifetime of the bilayers in micropores (from a few minutes to a few hours).[89] BLMs microdevices have been developed through standard micromachining techniques, creating apertures ranging from micro- to nano-sized in various

materials,[12c] including silicon,[29a, 90] glass,[91] silicon nitride,[92] silicon dioxide membranes, alumina substrates, and polymers such as Teflon,[32b, 93] PMMA,[29d, 94] and PDMS.[95]

The first automated BLMs-on–a-chip approach was presented by Suzuki *et al*..[29a] In this approach, the BLMs was formed at an etched aperture of a silicon substrate with flow channels on both sides. Lipid solution and buffer, injected alternatively, led to the formation of the BLMs. However, drawbacks associated with silicon-based devices, including high cost, low resistivity, and large shunt capacitances, prompted the research towards BLMs in polymeric devices.[11b, 29c] The silicon design was optimized towards a PMMA device, which allowed simultaneous formation of four bilayers in a single device with high reproducibility.[60] Sandison *et al*. employed hot embossing and laser micromachining to fabricate microfluidic channels in an air-exposed approach on PMMA-coated glass substrate.[29d] The upper chamber is filled with buffer and then drained to produce a thin lipid film, which is used to create a BLMs with a tick plug of lipid solution surrounding the aperture. As the two interfaces continue to drain, lipid monolayers come into contact, originating a bilayer. As the bilayer spans most of the aperture, fresh buffer is injected into the upper well to stabilize it.[29d]

Recognizing the advantages of PMMA microdevices and aiming to address the disadvantages of the painting method, Tomoike *et al*.[29e, 32c] developed a rotational chamber that emulates the painting method on a PMMA fluidic channel separated by a parylene micropore to repetitively form BLMs (**Figure 6A**). The microfluidic channels and chamber are pre-filled with an aqueous solution, and then a lipid/oil layer is painted over the micro-apertures on the basal part where the rotational chamber is fixed by the insertion of stoppers.[29e, 32c] Through cyclic motion, the aqueous solution from the chambers contacts the aqueous solution from the microfluidic channels at the micropores, forcing the formation of a second lipid monolayer. As the two lipid monolayers move closer, the oil portion becomes thinner, resulting in the formation of BLMs.[29e, 32c]

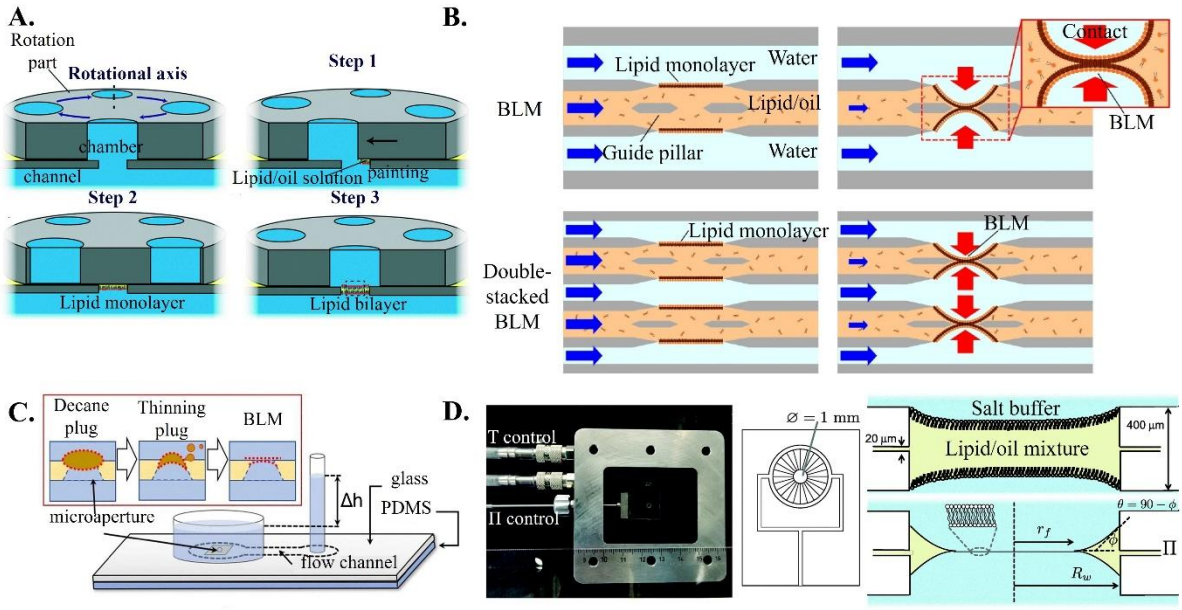


Figure 6. Formation of BLMs *in microfluidics* using different approaches. A) Rotational chambers on fluidic channels for repetitive formation of BLMs. Reproduced with permission.[29e] Copyright 2016, Royal Society of Chemistry. B) Formation of single or stacked BLMs through droplet contact method guided by pillars. Reproduced with permission under the terms of the CC-BY 4.0 license. [64] Copyright 2018, the Authors. Published by MDPI. C) Diagram of the BLMs formation illustrating the operating principles of hydrostatic pressure application, pressure-induced organic solvent plug thinning and final BLMs formation. Reproduced with permission.[32a] Copyright 2006, American Chemical Society. D) The bike wheel microchip channel geometry developed to obtain BLMs. Reproduced with permission.[66] Copyright 2016, Royal Society of Chemistry.

PMMA was also employed as substrate of a microfluidic device developed by Wang *et al*.[29b] for the insertion of proteins into BLMs formed over an aperture in a parylene film. In the reported configuration, the process involves filling both upper and lower chambers with buffer, followed by injection of lipid solution into the upper channel, which passes through onto the nanopores surface. At this stage, the lipid molecules organize at the n-decane/buffer interface. Finally, the buffer is sequentially introduced into the upper channel, leading to the formation of the bilayer.[29b] The sequential injection of buffer/lipid solution/buffer was also employed to reconstitute an array of lipid bilayers using parallel microchannels with numerous microchambers in their walls.[63] Due to the flow of the final injected buffer and the adsorption of organic solvents into PDMS, the membrane covering the microchamber thins

down, becoming a lipid bilayer.[63] In a similar architecture, Osaki *et al*.[61] integrated two functions into one single device: electrical input/output and optical imaging.

The wide use of polyether ether ketone (PEEK) in biomedical applications due to its unique properties (e.g., resistance to a wide range of chemicals and radiation, excellent barrier properties, electrical stability, and low protein adsorption),[65] has led to the development of a PEEK-based microfluidic device for studying protein-mediated ion flow across lipid membranes.[65] The creation of nanopores in PEEK foils was achieved by applying a picosecond pulsed laser, and BLMs were formed across these micropores in the microchannel.[65] Mayer *et al*. demonstrated the potential of Teflon AF films with multiple microfabricated pores for the stable formation of multiple BLMs at defined locations using the method of Montal and Mueller (1972).[93] Nonetheless, the microfabrication method for Teflon AF pores involves multiple steps over a period of hours due to the bulkiness of the material. To address this, micropores were made on ethylene tetrafluoroethylene (ETFE) using a microdrill with a heated tip. Then, BLMs were created on these apertures by painting an organic lipid solution with air bubbles generated at the tip of a pipette.[32b] In a different approach, represented in **Figure 6B**, BLMs were formed based on the strategy of lipid monolayer contacting. Two droplets, each surrounded by a lipid monolayer, enter into contact in a process guided by pillars.[64] The five-layered microchannel device comprises five inlets and outlets, a confluent area joining all channels, and pillar guides. Aqueous and lipid/oil solutions flow in each channel, forming three layers with aqueous solution alternated with two layers with lipid/oil solution in the confluent area.[64] At each one of the two lipid/water interfaces, a lipid monolayer spontaneously forms. By reducing the flow pressure of the lipid/oil layers, the monolayers come into contact, forming BLMs. The guide pillars serve a dual function: guiding the lipid/oil solution along their surface and serving as the aperture for the contact area of the two monolayers. The authors achieved the formation of a double-stacked BLMs through the manipulation of hydrostatic pressure.[64] The manipulation of hydrostatic pressure towards the formation of BLMs was also employed in an automated manner by Dugger *et al*. (**Figure 6C**).[32a] The authors developed an algorithm to manipulate the application of hydrostatic pressure within the microfluidic system controlled by feedback via confocal fluorescence monitoring.[32a] BLMs with large millimetric area were produced using a bikewheel-like chip encompassing a central annulus with 24 radially extended microchannels connecting to a larger channel (**Figure 6D**).[66] The BLMs formation in the center of the bikewheel orifice start with a thick film of lipid/oil surrounded by an aqueous buffer, which imposes a uniform hydrostatic pressure on the lipid layer. The pressure

increased slightly to initiate the controlled drainage of the thick film. As the lipid/oil mixture thinned by oil exclusion, a BLMs is nucleated and grew to form a circular film in the central annulus of bikewheel.[66]

3.2.4. Free-standing lipid bilayers

Free-standing lipid bilayers (FsLBs) were developed by Malmstadt *et al*.[30] by exploiting the characteristics of PDMS, particularly the propensity of organic solvents to partition into the hydrophobic elastomer, removing them from the fluidic stream. When a droplet of lipids in an organic solvent is introduced into an aqueous stream of a microfluidic device, lipids self-assemble at the solvent/aqueous interface. As the organic solvent are absorbed by the PDMS walls, the two lipid/water interfaces approach each other, resulting in the formation of a FsLBs.[30] This approach was also employed in other microfluidic setups. Heo *et al*.[67] described a PDMS device fabricated by 3D-printing containing two crossed channels separated by a horizontal FsLBs (**Figure 7A**). A SUVs suspension was used to generate asymmetric FsLBs, whereas a squalene lipid solution was employed to produce symmetric FsLBs. The fabrication of horizontal FsLBs involve trapping a droplet of squalene in the hole between the crossed channels, promoting the spread of a lipid monolayer at the squalene/buffer interface. Then, as squalene is removed by absorption into the PDMS, the two spontaneously come into contact, and horizontal FsLBs are formed in the hole.[67]

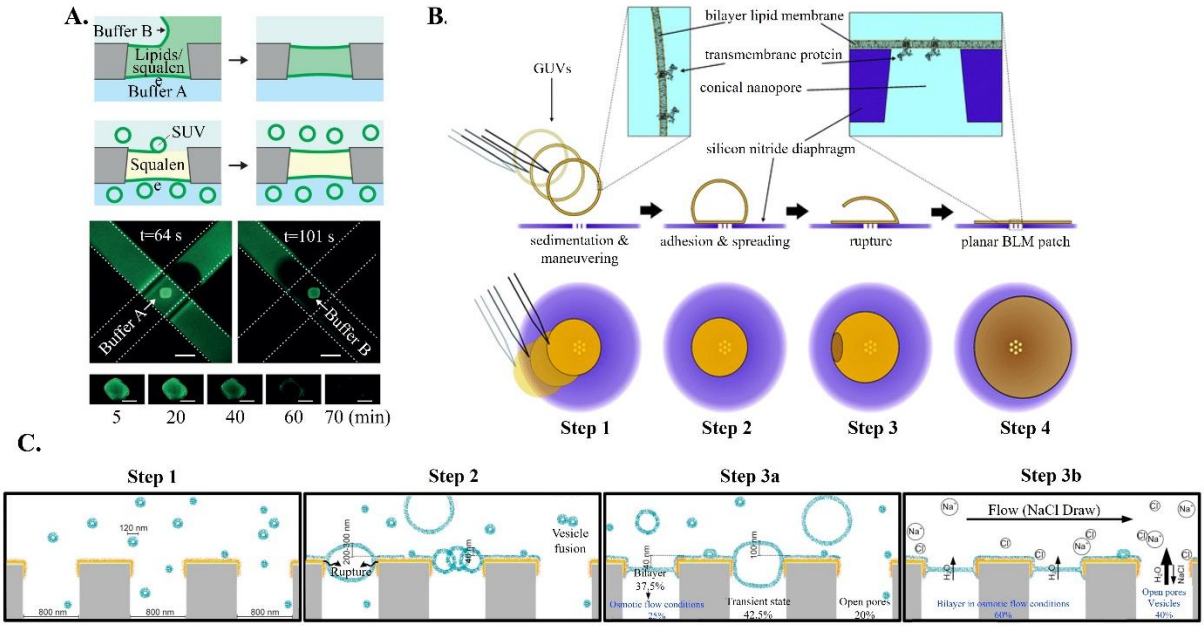


Figure 7. Approaches described to form FsLBs (A) and PsLBs (B – C) *in microfluidics*. A) Two methods for lipid monolayer formation: lipid-in-oil (upper scheme) and small

unilamellar vesicles-in-oil (bottom scheme) to form FsLBs and video frames of the initial filling the chip with lipid/squalene mixture than is pushed away by a buffer at the bottom and temporal sequential of PDMS absorbing squalene. Reproduced with permission.[67] Copyright 2019, Wiley. B) Schematic of PsLBs formation by directed fusion of a GUVs to a silicon nitride diaphragm containing an array of pores. Reproduced with permission.[28b] Copyright 2009, Royal Society of Chemistry. C) Proposed mechanism to form a hybrid membrane by vesicle fusion on a porous substrate, controlled by a previously formed lipid monolayer. Reproduced with permission.[28c] Copyright 2017, Elsevier.

3.2.5. Pore-suspensed lipid bilayers

Pore-suspensed lipid bilayers (PsLBs) can be described as bilayers covering a porous substrate, extending over both apertures and the 'solid' parts. In an approach similar to vesicle fusion, the direct fusion of GUVs over a silicon nitride diaphragm containing an array of pores were presented.[28b] A GUVs suspension is injected into the bathing electrolyte, and GUVs are sedimented and maneuverer by horizontal movements of a patch pipette tip attached to a micromanipulator, so one of them sinking at the pore-bearing (**Figure *7*B**).[28b] Upon contact, GUVs stick to the surface and spread out, covering the array pores. Further spontaneous local loss of integrity leads to rupture, which occurs at the GUV's border as it flattens on the surface. Once the vesicle unfolds, the defects gradually spread, and when completely unfolded, PsLBs spanning all pores of the array are formed.[28b] The main limitation of manual manipulation of lipid vesicles is the impediment for the process scalability. In a protocol inspired by the electroformation, Kuribayashi *et al*.,[28a] produced dome-shaped solvent-free PsLBs over an array of microapertures.[28a] This technique enabled the PsLBs formation with the ability to exchange solution through the aperture without the use of solvents, eliminating the need for precise control over the placement of pre-formed vesicles onto apertures. The size of the dome-shaped bilayers was determined by the initial size of the dried lipid film.[28a] Another approach to obtain PsLBs involves using a patterned solid substrate with solid posts coated with lipid monolayers, supporting the subsequent formation of lipid bilayers over nanopores existing between posts (**Figure *7*C**).[28c] The creation of such lipid assemblies occurs through vesicle fusion in three steps. Firstly, the thiolated gold-coated polycarbonate track-etched substrate is exposed to extruded vesicles. Secondly, some of these vesicles aggregate and fuse, resulting in giant vesicles that can block the pore entrance, while others fuse on the surface of the substrate, forming a monolayer.

Finally, the giant vesicles blocking the pores flatten to a disk-like structure until rupture at the contact line between their own lipids and the previously formed monolayer lipids, ultimately resulting in PsLBs. The PsLBs formation process takes approximately 8.5 hours, with the incubation time being crucial for the stability of the membrane.[28c] However, this approach requires further optimization in terms of reproducibility, as atomic force microscopy (AFM) micrographs of different parts of the same substrate show incomplete PsLBs formation, transient states and some open pores.[28c]

3.2.6. Droplet Interface Bilayers

Droplet interface bilayers (DIBs) are lipid bilayers formed when two lipid monolayer-coated aqueous droplets are brought in contact within an oil phase (**Figure 1E**).[31a, 96] This concept was proposed by David Needham in 2005 and developed in parallel by Funakoshi and coworkers, as an alternative method for bilayer formation without apertures.[15c, 97] Two microfluidic configurations in PMMA plastic plates were demonstrated. A 'double well chip' with two overlapping wells, where two water droplets are injected into each well already filled with lipid solution, and a 'cross-channel chip', combining two syringe pumps at the cross-section of two microchannels. A parylene layer was deposited between PMMA plates to prevent swelling due to solvent absorption. Capacitance measurements confirmed the formation of DIBs in both configurations.[97] Later, the authors proposed an optimized droplet-based lipid bilayer capable of exchanging the solution in a droplet while maintaining stable bilayers.[68] This optimization involved solution exchange through two microchannels placed under a well to form DIBs.[68] They further developed an automated microfluidic device for creating complex 3D network of DIBs (**Figure *8*A**).[31a] This platform facilitated the generation of droplets in a linear sequence with alternating compositions. A syringe pump in refill mode draw the liquid through thin PTFE tubing, and the tubing tip was alternatively moved between oil and vesicle solutions using a two-channel autosampler to create vesicle droplets and pump them into a glass channel.[31a]

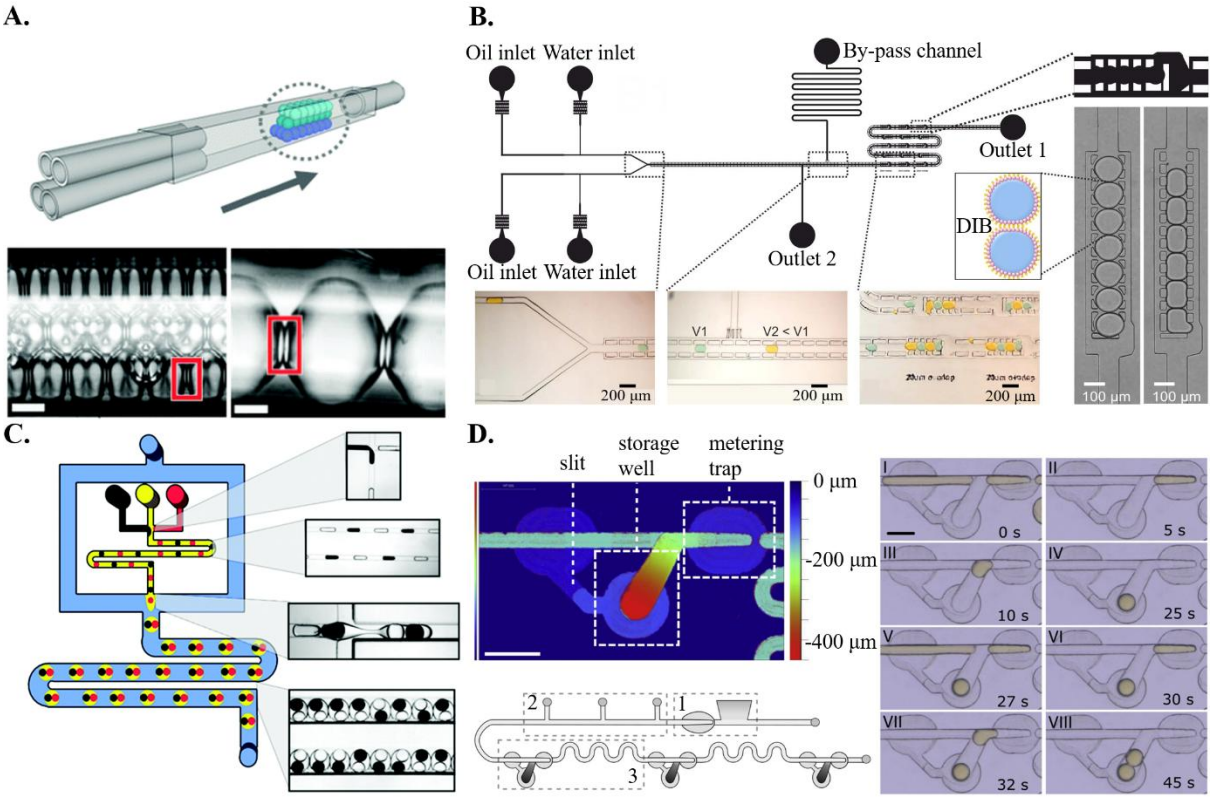


Figure 8. Formation of droplet interface bilayers (DIBs) *in microfluidics*. A) Schematic of the experimental set-up constituted by a PTFE tubing to form DIBs network. Reproduced with permission.[31a] Copyright 2010, Royal Society of Chemistry. B) Schematic drawing of a microfluidic device developed to form DIBs in a computer-controlled format. Reproduced with permission under the terms of the CC-BY 4.0 license.[14] Copyright 2015, the Authors. Published by Springer Nature. C) Schematic of a microfluidic device and corresponding bright field images of different regions to generate DIBs-based multisomes. Reproduced with permission under the terms of the CC-BY 3.0 license.[31b] Copyright 2016, the Authors. Published by Royal Society of Chemistry. D) Design and operation of a Meter&Store module to form DIBs, including a profilometry scan depicting the architecture of microfluidic trap. Reproduced with permission.[72] Copyright 2019, Elsevier.

The DIBs formation approach boasts two key features: (i) the use of nanosized lipid-stabilized W/O droplets that minimize costs; and (ii) a computer-controlled microfluidic network for fast and reconfigurable start/stop experimentation (**Figure *8*B**).[14] An arraying format of DIBs was employed to create a platform integrating the formation of lipid-stabilized W/O droplets with precise positioning.[14] For asymmetric bilayer formation, DIBs with different lipid compositions can be alternately produced (e.g. ABAB). When a droplet encounters another, a bilayer with a different lipid composition in each leaflet is formed.[69] Introducing a

stepping motor in a microfluidic device allowed the generation of an asymmetric lipid bilayer through DIBs carrying different lipid compositions.[70] The DIBs formation method was also used to generate multisomes in a microfluidic device with two sequential droplet generation modules separated by a meandering channel (**Figure *8*C**).[31b] At the first junction, W/O droplets with alternating compositions were produced due to the two opposing T-junctions format. The traveling of the droplets through the meander enabled bilayers to form at the droplet-droplet interface, preventing coalescence upon encountering the outer aqueous phase. At the second junction, in flow-focusing geometry, a set number of aqueous droplets are encapsulated in larger oil droplets, yielding multisomes. The size and architecture of these multisomes depended on device geometry, flow rates and frequency.[31b] A more complex strategy to address the mass transport phenomenon involved a flow-focusing geometry system of two drops that flow in two channels and interact through a pore.[15d] The Meter&Store unit, comprising a metering trap and an adjacent store, offers a simpler and less intervention-intensive approach. Scaled down to operate on droplets with volumes as small as 9 nL, it was incorporated into a microfluidic chip capable of rapidly producing DIBs pairs with controlled chemical composition (**Figure *8*D**).[72] After a droplet is produced in the continuous flow, it encounters the metering trap (a barrier obstructing the channel and a set of bypasses). If the droplet is larger than the trap, the rear aligns with the entrance to the bypasses, and the oil starts to flow around the droplet. The droplet is then split at the barrier into two portions: one with a well-defined volume is locked in the trap, and the remaining part is pushed into the main channel.[72] As the continuous flow in the main channel stops, the trapped droplet flows spontaneously back to the storage well by capillary forces. The interface of a pair of droplets linked in storage wells forms a bilayer, and successful bilayer formation is monitored by changes in reflected light.[72] To achieve a tighter arrangement of droplets and create a honeycomb pattern in a 2D space resembling epithelial tissues, the interfacial tension of lipid droplets was adjusted by introducing surfactants with higher adsorption rates. The microfluidic device designed for this purpose consists of two sections: while in the first section the droplets are generated through a flow-focusing mechanism, in the second section they are captured and arranged in a U-shape chamber.[71]

4. Lipid biomimetic models on-chip for drug discovery applications

Lipid biomimetic models in microfluidic devices have found applications in drug-membrane interaction screening. Considering the main scope of this review, the applications will be

divided on lipid microfluidic biomimetic models for permeation and/or partition screening and for analysis of drug effects on membrane biophysics.

4.1. Lipid microfluidic biomimetic models for drug permeation and/or partition screening

Cell membrane serves as the primary barrier between intracellular and extracellular environments, and the exchange of molecules across this boundary is governed by the lipid bilayer. Predicting the movement of chemical entities through this physiological barrier is of great importance in drug discovery process. Therefore, various microfluidic technologies have been developed to enhance the throughput of screening assays in this context (Table 4).

Table 4. Summary of lipid microfluidic biomimetic models for drug permeation/partition screening applications.

Lipid Model	Lipid Composition	Device Material	Experimental Techniques	Aims	Ref.
Immobilized lipid vesicles	POPC and human aquaporin-POPC	PDMS	TIRF microscopy	Monitor the transport of uncharged solutes across bilayer through a pH-sensitive dye.	[98]
Immobilized lipid vesicles	DPPC:DOPC:Chol (1:1:1)	PDMS	SDCM	Analysis of the impact of increasing number of carboxylic acids on membrane permeability.	[99]
Immobilized lipid vesicles	DPPC:DOPC:Chol (1:1:1)	PDMS	SDCM	Evaluation of the effects of ethylene oxide units on PEG-NBD permeation through lipid bilayers.	[100]
Immobilized lipid vesicles	DLPC:POPG:Chol	PDMS	TIRF microscopy	Determination of the permeation coefficient of tetracyclines to support chemical modifications.	[101]
Lipid vesicles	DOPG:DOPC (1:3)	PDMS	UV Epifluorescence	Study of membrane permeability of two antibiotics (norfloxacin and ciprofloxacin) across a bacterial biomimetic membrane.	[102]
Lipid vesicles	DPhPC	PDMS	Electrical Impedance	Monitoring the antibiotic permeation across lipid bilayers.	[103]
Lipid vesicles	POPC:Chol (9:1)	PDMS	Confocal Microscopy	Determine the water permeability of a lipid bilayer.	[104]

SLBs	SOPC:b-X-DPPE:TR-DPPE	Si	X-Ray reflectivity, fluorescence microscopy and FRAP	Characterization of protein-membrane interactions.	[37]
SLBs	POPC:SM:Chol	PDMS	FRAP	Measurements of partitioning kinetics of membrane-bound species to or from different lipid phases.	[105]
DIBs	DOPC	PDMS	Fluorescence microscopy, UV-Vis microspectroscopy	Evaluation of the effective permeability of fluorescein and caffein from the donor to the acceptor droplets.	[106]
DIBs	DPhPC and DOPC	Polycarbonate	Fluorescence microscopy	Quantification of small molecules permeation through lipid bilayers.	[72]
DIBs	PC:PE:SM:Chol	PDMS	Fluorescence microscopy	Explore the influence of asymmetric membranes on DOX pharmacokinetics.	[107]
DIBs	Asymmetric DOPC/DOPE:DOPS (3:7)	Glass	Fluorescence microscopy and LC-MS analysis	Explore the potentiality of symmetric and asymmetric DIBs array for permeability studies (rhodamine used as model molecule)	[108]

Abbreviations: b-X-DPPE – n-((6-(biotinoyl)amino)hexanoyl)-dipalmitoylphosphatidylethanolamine triethylammonium salt; Chol – cholesterol; DIBs – droplet interface bilayers; DLPC – dilauroylphosphocholine; DOPC – dioleoylphosphatidylcholine; DOPE – dioleoylphosphatidylethanolamine; DOPG – dioleoylphosphatidylglycerol; DOPS – dioleoylphosphatidylserine; DOX – doxorrubicin; DPhPC – diphytanoylphosphatidylcholine; DPPC – dipalmitoylphosphatidylcholine; FRAP – fluorescence recovery after photobleaching; PDMS – polydimethylsiloxane; PEG-NBD - poly(ethylene glycol)-nitrobenzoxadiazole; POPC – palmitoyloleoylphosphocholine; POPG – palmitoyloleoylphosphatidylglycerol; SDCM – spinning-disk confocal microscopy; Si – silicon; SLBs – supported lipid bilayers; SM – sphingomyelin; SOPC – stearoyloleoylphosphocholine; TIRF – total-internal reflection microscopy; TR-DPPE – dihexadecanoylphosphoethanolamine triethylammonium salt.

Kuyper *et al*.[109] employed total-internal reflection (TIRF) microscopy and rapid buffer exchange *in microfluidics* to investigate proton permeation across lipid bilayers. It was observed a two-step mechanism comprising a transient pore and a solubility-diffusion, by

using carboxyfluorescein, a pH-sensitive dye, encapsulated into immobilized POPC LUVs.[109] Dynamic light scattering (DLS) was used to characterize the LUVs, revealing a high polydispersity.[109] Malmsttadt *et al.* immobilized GUVs using biotin-streptavidin interaction to monitor the permeation of PEGs with different lengths across membranes via spinning-disk confocal microscopy.[100] The same system was later used to measure the permeation of unlabeled carboxylic acids into immobilized GUVs using a pH sensitive dye.[110] As expected, more lipophilic molecules permeated the membrane more rapidly than less lipophilic ones.[100, 110] A similar set up allowed to measure the permeation of acetic acid into single carboxyfluorescein-filled LUVs with fast buffer exchange, on the sub 100 ms scale.[98] This latter set up presented an automatic liquid handling compatible with subsequent measurements using different solution exposed to the same set of surface-immobilized lipid vesicles. These advantages not only reduce the sample conditions, as fastens the search through huge compound libraries for the most promising drug compounds.[98] A PDMS microfluidic device was employed to monitor the kinetics of tetracycline permeation on immobilized LUVs by TIRF microscopy, allowing parallel analysis of different conditions. Another PDMS device sandwiching a polycarbonate membrane coated with a lipid mixture was developed to analyze percutaneous permeability.[111] This approach presented improved throughput, compared to typical sized diffusion cells through an online detection approach, which enhances the data acquisition rate without perturbing the system with sampling. Although this setup provides an opportunity to use accessible techniques, there is a dearth of information regarding the characterization of the lipid model sprayed on polycarbonate membranes.

An optofluidic permeability assay was designed to assess the permeability coefficient of electroformed GUVs to autofluorescent fluoroquinolone drugs, adopting a label-free approach.[112] The internalization in GUVs was quantified using a UV epifluorescence microscope designed for this purposed.[112] The system underwent further enhancement with the integration of an OLA unit, allowing both the continuous production and screening of lipid vesicles on a single device for several hours.[102] The optimized platform was subsequently employed to monitor the permeation of norfloxacin and ciprofloxacin through biomimetic bacterial membranes under physiological and salt concentrations, allowing to perform up to 11 experiments consecutively.[102] Although OLA unit integration into the system leads to improved throughput of lipid vesicles production, the permeability experiment throughput still limited by the camera speed.[102, 112]

DIBs found application in reconstituting the parallel artificial membrane permeability assay (PAMPA) within a microfluidic platform.[106] PAMPA is a widely used method in pharmaceutical research for the rapid determination of permeability through passive transport across membranes placed between top and bottom wells, typically conducted in multi-well plates.[106] In their approach, Nisisako *et al.* used an array of alternating donor and acceptor DIBs, created in cross-flowing oil containing lipids, to replace the conventional membrane PAMPA. Subsequent removal of the oil through hydrophobic pseudo-porous sidewalls facilitated the contact between two stationary DIBs. The permeation of chemicals across the DIBs was conducted on and ABAB droplet array and monitored by UV-Vis and/or fluorescence techniques at different time points, relying on previously established calibration data and the measured concentration in the DIBs acceptor.[106] Comparing with the conventional PAMPA assay, this DIBs array approach was able to quantify the permeation of compounds in 10-20 minutes, significantly shorter time range. Additionally, DIBs were employed to assess permeation rates through a lipid bilayer formed for two trapped droplets using fluorescence microscopy to monitor the concentration changes.[72]

4.2. Lipid microfluidic biomimetic models for screening drug effects on membrane biophysical characteristics

The reciprocal interaction between drugs and cell membranes can significantly influence the biophysical structure and function of membranes. Predicting the potential effects of a drug candidate on lipid membranes is essential for toxicity prediction. Table 5 summarizes the reported microfluidic applications for drug membrane biophysical effects.

Table 5. Summary of lipid microfluidic biomimetic models for screening of the effects on the drug on the biophysical characteristics of the membrane.

Lipid Model	Lipid Composition	Device Material	Experimental Techniques	Aims	Ref.
SLBs Array	eggPC:DOPS	Glass	Fluorescence microscopy	Characterization of nimesulide effects on lipid bilayer fluidity.	[56]
SLBs Array	eggPC:DOPS	Glass	Fluorescence microscopy	Screening fluorescently-labelled annexin A5 binding to a DOPS concentration gradient.	[113]
SLBs	POPC:Chol and POPE:POPG	Conductive Polymer/PEDOT:PSS	QCM-D and EIS	Evaluation of the effects caused by a bacterial toxin	[58]

				and an antibiotic compound on lipid bilayers.	
SLBs	DPPC	PDMS	FRAP	Determination of lipid phase transition on a linear temperature gradient generated across parallel microchannels simultaneously.	[114]
BLMs	DOPC, POPG, DPPC and Chol (single or varying compositions)	Aluminum	Optical and confocal microscopies	Characterization of the interaction between an amphiphilic triblock polymer F68 and lipid biomimetic models.	[66]
PsLBs	DOPC, DOPC:DOPG (3:1), DOPC:DOPS (3:1), DOPC:DOPG:DOPE (2:1:1)	PDMS	FLCS and EIS	Characterization of the interaction between a series of nonsteroidal anti-inflammatories in biomimetic models.	[7a]
Lipid vesicles	DOPC:DPPC:Chol (7:7:6)	PDMS and glass	Fluorescence microscopy	Exploration of the pore-forming antimicrobial peptide melittin's lipid interaction dynamics using a mammalian membrane model.	[19]
Lipid vesicles	DOPC and SM:DOPC:Chol	PDMS	Microscopy	Observation of domain reorganization in mechanically compressed GUVs.	[115]
FsLBs	DOPC:DOPE (3:1)	PDMS	Confocal microscopy, FRAP and surface tension	Investigation of the ADRP effect on lipid diffusion properties.	[116]

Abbreviations: Chol – cholesterol; DOPC – dioleoylphosphatidylcholine; DOPE – dioleoylphosphatidylethanolamine; DOPG – dioleoylphosphatidylglycerol; DOPS – dioleoylphosphatidylserine; DPPC – dipalmitoylphosphatidylcholine; eggPC – egg phosphatidylcholine; EIS – electrochemical impedance spectroscopy; GUVs – giant unilamellar vesicles; FLCS – fluorescence lifetime correlation spectroscopy; FRAP – fluorescence recovery after photobleaching; PDMS – polydimethylsiloxane; PEDOT:PSS – poly(3,4-ethylenedioxythiophene) polystyrene sulfonate; POPC – palmitoyloleoylphosphocholine; POPE – palmitoyloleoylphosphatidylethanolamine; POPG – palmitoyloleoylphosphatidylglycerol; QCM-D – quartz crystal microbalance with dissipation monitoring; SLBs – supported lipid bilayers; SM – sphingomyelin.

A stamped array of SLBs through hydrogel stamping was employed to screen the interactions of the protein Annexin A5 with a range of lipids, including bilayers containing up to 50% negatively-charged lipids and cholesterol.[56, 113] This setup provided a rapid means to study the effects of various conditions in parallel. A microfluidic platform comprising 14 parallel microchannels coated with SLBs through vesicle fusion method was developed to study the phase transition temperature of DPPC bilayers.[114] The channels were exposed to a temperature gradient from 22 to 51 °C by flowing hot and cold solutions next to the area of interest. Each SLBs in each channel was subjected to the temperature gradient, and fluorescence recovery after photobleaching (FRAP) was employed to determine lipid diffusion, which changes at the phase transition temperature.[114] Although this setup specifically targeted DPPC transition temperature, it presents an opportunity to study the effects of molecules on such transitions, providing insights into biophysically induced changes in membranes. In another microfluidic platform integrating SLBs, FRAP studies were employed to measure the association/dissociation kinetics of biomolecules into different lipid membrane phases (liquid-ordered raft phase with cholesterol or liquid-disordered with unsaturated lipids).[105] Two regions were patterned by laminar flow using vesicle fusion method inside the microchannel, and biomolecules were subsequently introduced.[105] Microcavity SLBs, as described in previous section, were employed to evaluate the drug-membrane interaction of seven different drugs, including nonsteroidal anti-inflammatories, antibiotics and bisphosphonates.[7a] Fluorescence lifetime correlation spectroscopy (FLCS) and electrochemical impedance spectroscopy (EIS) measurements were performed to evaluate the impact of the drugs on single, binary and ternary bilayers over physiologically relevant drug concentrations.[105] The reported data were consistent with the literature, indicating that microcavity SLBs can be a promising approach to study drug interaction with physiological relevant membranes.[7a] The interaction between the antimicrobial peptide melittin (AMP) and typical mammalian biomimetic GUVs model was evaluated in a platform combining fluorescence microscopy analysis with GUVs formation by electroformation.[19] While through conventional single GUVs techniques, typical dye-leakage experiments allow data acquisition from less than 10 individual vesicles, the integrated microfluidic analysis proposed allowed the simultaneous data acquisition from over 80 GUVs in one single experiment.[19]

SLBs formed by the SALB method were used to evaluate the biophysical effect of a bacterial toxin (α-hemolysin) and an antibiotic compound (polymyxin B) in SLBs mimicking the lipid

composition of mammalian and bacterial cell membranes, respectively.[58] The interactions were monitored through quartz crystal microbalance with dissipation monitoring (QCM-D) and EIS techniques.[58] A significant decrease of frequency and resistance measured through QCM-D and EIS, respectively, were associated with the pore formation caused by α-hemolysin on the mammalian model. Additionally, the loss of membrane integrity caused by polymyxin B is supported by an increased frequency as the SLBs material disappeared from the surface and by significant reduction in the resistance of the SLBs.[58] The bikewheel setup, consisting of a circular BLMs in the center annulus, was employed to evaluate the interaction of the FDA-approved amphiphilic triblock polymer F68 (PEG40-PPO27-PEG40) with membranes.[66] This polymer, known as 'membrane sealant' promising to Duchenne muscular dystrophy, was studied for its effects on membrane tension. Regular and confocal microscopies were applied to the described system to monitor membrane tension changes induced by F68, which were associated with variations in lipid packing around the polymer.[66]

5. Final remarks and future outlook

This review emphasizes the relevance of studying drug-membrane interactions towards a comprehensive molecular understanding of the pharmacological properties of a chemical entity. Investigations into the interaction between drug molecules and cell membranes have demonstrated a good correlation between biophysical interactions and cellular uptake and/or therapeutic efficacy. Regarding this, insights into the membrane biophysical modifications due to drug interactions can guide the design of more effective therapeutic bioactives coupled with tuned toxicity profiles. The use of whole cell models for a systematic evaluation of the influence of drugs on membrane properties is challenging and not suitable for routine screening. Biomimetic lipid model membrane systems offer an alternative platform to natural membranes, allowing the study of such interactions under very defined and controlled conditions, often incompatible with viable live cells. Lipid bilayers mimicking cell membranes can be formed in several architectures that have been extensively characterized and analyzed using a wide range of biophysical techniques. Therefore, selecting the most appropriated methodology and architecture is essential for this research focus. Actually, some of the model membrane platforms provide overlapping information, but the specific type of model dictates the applicable characterization techniques.

Considering the demands of the pharmaceutical industry for high throughput screening (HTS) solutions, microfluidic technology represents a promising avenue to address challenges in

lipid biomimetic models for screening applications. Microfluidic science allows massive test parallelization and facilitates the integration of laboratory procedures into planar chips, reducing reaction volumes and associated costs while enhancing throughput and analytical performance. Artificial cell membranes, based on microfluidic solutions, have been explored on various substrates like glass, silicon, and polymers, employing diverse self-assembly approaches. While microfluidics holds great promise for producing lipid models with controlled properties, the reproducibility and practicality of these methods vary widely. Notably, even within microfluidic platforms, the predominant use involves supported lipid bilayers (SLBs) and lipid vesicles, which can be attributed to the increased stability of these lipid biomimetic models. Notwithstanding, a clear droplet interface bilayers preference is beginning to be noticed. In microfluidic devices, lipid vesicles are often immobilized on solid supports, allowing for high-throughput experiments and the utilization of surface-sensitive techniques for detection. The combination with microfluidics facilitates rapid solution exchange for kinetic studies and volume reduction. Conversely, SLBs are formed through various approaches, all rooted in the conventional vesicle fusion method. Despite the diverse and elegant approaches for forming different lipid bilayers *in microfluidics*, these techniques seem underutilized in drug screening. Instead, most described approaches focus on nanocarrier development for drug encapsulation.

From our perspective, array formats of lipid bilayers are particularly promising for drug screening, enabling simultaneous experiments and HTS of compound libraries. Various techniques are employed to form lipid bilayer arrays, including the deposition of lipid vesicle suspension droplets onto surfaces, vesicle fusion onto patterned substrates, and microcontact printing using polymeric stamps. As no singular system design or material has been shown to be superior, a variety of solutions have been suggested and should be evaluated based on the intended applications. Nevertheless, to harness the full potential of microfluidic platforms, validation of these assays and evidence of their reliability compared to conventional assays are crucial.

To our knowledge, drug-membrane interaction studies on microfluidic systems are currently inconclusive, and while the number of reported approaches is expected to increase, systematic characterization of lipid models produced by each approach is required before they can replace the conventional, but well characterized lipid models, in membrane interaction studies. Additionally, pharmaceutical industries demand standardization in drug candidates profiling towards a faster yet effective drug screening at early phases of drug discovery.

Acknowledgements

This work was supported by the Portuguese Foundation for Science and Technology (FCT) under strategic funding in the framework of the Strategic Programs UID/FIS/04650/2020, UIDB/04436/2020, UIDP/04436/2020. E.F. thanks also the FCT for the SFRH/BD/147938/2019 grant and VC for the contract under the Stimulus of Scientific Employment 2020.02304.CEECIND. The authors also acknowledge funding by the Department of Education of the Basque Government (PIBA program, Grant number 2022333047), from the Basque Government Industry Department under the ELKARTEK program, and by the Spanish Ministry of Science and Innovation (Grant number PID2022-138572OB-C42).

Received: ((will be filled in by the editorial staff))

Revised: ((will be filled in by the editorial staff))

Published online: ((will be filled in by the editorial staff))

References

[1] a) D. Lombardi, P. S. Dittrich, *Expert Opin. Drug Discovery* **2010**, 5, 1081; b) K. H. Bleicher, H. J. Bohm, K. Muller, A. I. Alanine, *Nat. Rev. Drug Discovery* **2003**, 2, 369.

[2] J. Hodgson, *Nat. Biotechnol.* **2001**, 19, 722.

[3] K. Richardson, K. Cooper, M. S. Marriott, M. H. Tarbit, P. F. Troke, P. J. Whittle, *Rev. Infect. Dis.* **1990**, 12 Suppl 3, S267.

[4] a) T. Hou, J. Wang, *Expert Opin. Drug Metab. Toxicol.* **2008**, 4, 759; b) M. H. Tarbit, J. Berman, *Curr. Opin. Chem. Biol.* **1998**, 2, 411.

[5] a) H. Li, T. Zhao, Z. Sun, *Reviews in Analytical Chemistry* **2018**, 37; b) A. M. Seddon, D. Casey, R. V. Law, A. Gee, R. H. Templer, O. Ces, *Chem. Soc. Rev.* **2009**, 38, 2509; c) M. Lucio, J. L. Lima, S. Reis, *Curr Med Chem* **2010**, 17, 1795; d) R. Bilginer, A. Arslan Yildiz, in *Biomimetic Lipid Membranes: Fundamentals, Applications, and Commercialization*, DOI: 10.1007/978-3-030-11596-8_10 **2019**, Ch. Chapter 10, p. 225.

[6] a) C. Peetla, A. Stine, V. Labhasetwar, *Mol. Pharmaceutics* **2009**, 6, 1264; b) J. K. Seydel, M. Albores Velasco, E. A. Coats, H. P. Cordes, B. Kunz, M. Wiese, *Quant. Struct.-Act. Relat.* **1992**, 11, 205.

[7] a) S. Ramadurai, N. K. Sarangi, S. Maher, N. MacConnell, A. M. Bond, D. McDaid, D. Flynn, T. E. Keyes, *Langmuir* **2019**, 35, 8095; b) D. Barata, C. van Blitterswijk, P. Habibovic, *Acta Biomater.* **2016**, 34, 1.

[8] a) H. Li, T. Zhao, Z. Sun, *Rev. Anal. Chem.* **2018**, 37, 1; b) J. Knobloch, D. K. Suhendro, J. L. Zieleniecki, J. G. Shapter, I. Koper, *Saudi J. Biol. Sci.* **2015**, 22, 714; c) M. Lúcio, J. L. F. C. Lima, S. Reis, in *Ideas in Chemistry and Molecular Sciences*, DOI: 10.1002/9783527630516.ch8 **2010**, p. 191.

[9] a) M. Lucio, J. L. Lima, S. Reis, *Curr. Med. Chem.* **2010**, 17, 1795; b) J. Sarkis, V. Vié, *Front. Bioeng. Biotechnol.* **2020**, 8, 270; c) E. Fernandes, S. Benfeito, F. Cagide, H. Gonçalves, S. Bernstorff, J. B. Nieder, M. E. Cd Real Oliveira, F. Borges, M.

Lúcio, *Nanotechnol. Sci. Appl.* **2021**, Volume 14, 7; d) E. Fernandes, T. B. Soares, H. Goncalves, M. Lucio, *Front. Chem.* **2018**, 6, 323.

[10] a) M. di Cagno, H. A. Bibi, A. Bauer-Brandl, *Eur. J. Pharm. Sci.* **2015**, 73, 29; b) H. A. Bibi, M. di Cagno, R. Holm, A. Bauer-Brandl, *Int. J. Pharm.* **2015**, 493, 192; c) A. C. Jacobsen, S. Nielsen, M. Brandl, A. Bauer-Brandl, *Pharm. Res.* **2020**, 37, 93; d) M. Falavigna, M. Klitgaard, C. Brase, S. Ternullo, N. Skalko-Basnet, G. E. Flaten, *Int. J. Pharm.* **2018**, 537, 213; e) A. Engesland, N. Skalko-Basnet, G. E. Flaten, *J. Pharm. Sci.* **2015**, 104, 1119; f) B. Sinko, T. M. Garrigues, G. T. Balogh, Z. K. Nagy, O. Tsinman, A. Avdeef, K. Takacs-Novak, *Eur. J. Pharm. Sci.* **2012**, 45, 698; g) A. Loidl-Stahlhofen, T. Hartmann, M. Schottner, C. Rohring, H. Brodowsky, J. Schmitt, J. Keldenich, *Pharm. Res.* **2001**, 18, 1782; h) L. M. Magalhaes, C. Nunes, M. Lucio, M. A. Segundo, S. Reis, J. L. Lima, *Nat. Protoc.* **2010**, 5, 1823.

[11] a) L. Kang, B. G. Chung, R. Langer, A. Khademhosseini, *Drug Discov. Today* **2008**, 13, 1; b) J. S. Kochhar, S. Y. Chan, P. S. Ong, W. G. Lee, L. Kang, in *Microfluidic Devices for Biomedical Applications*, DOI: 10.1533/9780857097040.2.231 **2013**, p. 231.

[12] a) P. S. Dittrich, A. Manz, *Nat. Rev. Drug Discovery* **2006**, 5, 210; b) Y. Elani, *Biochem. Soc. Trans.* **2016**, 44, 723; c) M. Zagnoni, *Lab Chip* **2012**, 12, 1026; d) Y. Dong, K. S. Phillips, Q. Cheng, *Lab Chip* **2006**, 6, 675; e) A. I. Neto, C. R. Correia, C. A. Custódio, J. F. Mano, *Adv. Funct. Mater.* **2014**, 24, 5096; f) N. Tabatabaei Rezaei, H. Kumar, H. Liu, S. S. Lee, S. S. Park, K. Kim, *Adv. Healthcare Mater.* **2023**, 12, e2203172.

[13] a) S. C. Terry, J. H. Jerman, J. B. Angell, *IEEE Trans. Electron Devices* **1979**, 26, 1880; b) G. M. Whitesides, E. Ostuni, S. Takayama, X. Jiang, D. E. Ingber, *Annu. Rev. Biomed. Eng.* **2001**, 3, 335; c) M. Alberti, Y. Dancik, G. Sriram, B. Wu, Y. L. Teo, Z. Feng, M. Bigliardi-Qi, R. G. Wu, Z. P. Wang, P. L. Bigliardi, *Lab Chip* **2017**, 17, 1625.

[14] B. Schlicht, M. Zagnoni, *Sci. Rep.* **2015**, 5, 9951.

[15] a) S. Matosevic, *Bioessays* **2012**, 34, 992; b) D. van Swaay, A. deMello, *Lab Chip* **2013**, 13, 752; c) H. Bayley, B. Cronin, A. Heron, M. A. Holden, W. L. Hwang, R. Syeda, J. Thompson, M. Wallace, *Mol. BioSyst.* **2008**, 4, 1191; d) Z. Hayat, *Biomed. J. Sci. & Tech. Res.* **2019**, 21, 15611; e) F. Mazur, M. Bally, B. Städler, R. Chandrawati, *Adv. Colloid Interface Sci.* **2017**, 249, 88.

[16] a) J. Ahn, J. Ko, S. Lee, J. Yu, Y. Kim, N. L. Jeon, *Adv. Drug Delivery Rev.* **2018**, 128, 29; b) V. Giridharan, Y. Yun, P. Hajdu, L. Conforti, B. Collins, Y. Jang, J. Sankar, *J. Nanomater.* **2012**, 2012, 1; c) A. Mansoorifar, R. Gordon, R. Bergan, L. E. Bertassoni, *Adv. Funct. Mater.* **2021**, 31, 2006796.

[17] M. Batool, B. Ahmad, S. Choi, *Int. J. Mol. Sci.* **2019**, 20, 2783.

[18] E. Rascol, J.-M. Devoisselle, J. Chopineau, *Nanoscale* **2016**, 8, 4780.

[19] D. J. Paterson, J. Reboud, R. Wilson, M. Tassieri, J. M. Cooper, *Lab Chip* **2014**, 14, 1806.

[20] M. Deleu, J.-M. Crowet, M. N. Nasir, L. Lins, *Biochim. Biophys. Acta, Biomembr.* **2014**, 1838, 3171.

[21] E. Fernandes, S. Benfeito, F. Cagide, H. Goncalves, S. Bernstorff, J. B. Nieder, M. E. Cd Real Oliveira, F. Borges, M. Lucio, *Nanotechnol., Sci. Appl.* **2021**, 14, 7.

[22] a) G. M. El Maghraby, A. C. Williams, B. W. Barry, *Int. J. Pharm.* **2005**, 292, 179; b) A. Ambrosini, G. Bossi, S. Dante, B. Dubini, L. Gobbi, L. Leone, M. Grazia Ponzi Bossi, G. Zolese, *Chem. Phys. Lipids* **1998**, 95, 37; c) E. Fernandes, T. B. Soares, H. Goncalves, S. Bernstorff, M. Real Oliveira, C. M. Lopes, M. Lucio, *Int. J. Mol. Sci.* **2018**, 19, 3411; d) A. M. Carvalho, E. Fernandes, H. Goncalves, J. J. Giner-Casares, S. Bernstorff, J. B. Nieder, M. Real Oliveira, M. Lucio, *Int. J. Pharm.* **2020**, 580,

119222; e) A. Almeida, E. Fernandes, B. Sarmento, M. Lucio, *Pharmaceutics* **2021**, 13, 869; f) M. Lucio, F. Bringezu, S. Reis, J. L. Lima, G. Brezesinski, *Langmuir* **2008**, 24, 4132; g) C. Pereira-Leite, C. Nunes, J. L. Lima, S. Reis, M. Lucio, *J. Phys. Chem. B* **2012**, 116, 13608; h) A. Wagner, K. Vorauer-Uhl, *J. Drug Delivery* **2011**, 2011, 591325; i) A. Akbarzadeh, R. Rezaei-Sadabady, S. Davaran, S. W. Joo, N. Zarghami, Y. Hanifehpour, M. Samiei, M. Kouhi, K. Nejati-Koshki, *Nanoscale Res. Lett.* **2013**, 8, 102; j) B. Maherani, E. Arab-Tehrany, M. R. Mozafari, C. Gaiani, M. Linder, *Curr. Nanosci.* **2011**, 7, 436.

[23] A. Gouda, O. S. Sakr, M. Nasr, O. Sammour, *J. Drug Delivery Sci. Technol.* **2021**, 61.

[24] a) Y. P. Patil, S. Jadhav, *Chem. Phys. Lipids* **2014**, 177, 8; b) C. Isalomboto Nkanga, A. Murhimalika Bapolisi, N. Ikemefuna Okafor, R. Werner Maçedo Krause, in *Liposomes - Advances and Perspectives*, DOI: 10.5772/intechopen.84255 **2019**, Ch. Chapter 3, p. 1; c) F. Inci, in *Biomimetic Lipid Membranes: Fundamentals, Applications, and Commercialization*, DOI: 10.1007/978-3-030-11596-8_9 (Ed: F. N. Kök) **2019**, Ch. Chapter 9, p. 213; d) S. Damiati, *Biomed. Microdevices* **2019**, 21, 62; e) T. Trantidou, M. Friddin, Y. Elani, N. J. Brooks, R. V. Law, J. M. Seddon, O. Ces, *ACS Nano* **2017**, 11, 6549; f) D. Lombardo, M. A. Kiselev, *Pharmaceutics* **2022**, 14.

[25] M. M. Velázquez, T. Alejo, D. López-Díaz, B. Martín-García, M. D. Merchán, in *Two-dimensional Materials - Synthesis, Characterization and Potential Applications*, DOI: 10.5772/63495 **2016**, Ch. Chapter 2, p. 21.

[26] a) T. K. Lind, M. Cardenas, H. P. Wacklin, *Langmuir* **2014**, 30, 7259; b) G. J. Hardy, R. Nayak, S. Zauscher, *Curr. Opin. Colloid Interface Sci.* **2013**, 18, 448.

[27] a) A. C. Simonsen, L. A. Bagatolli, *Langmuir* **2004**, 20, 9720; b) J. Kurniawan, J. F. Ventrici de Souza, A. T. Dang, G.-y. Liu, T. L. Kuhl, *Langmuir* **2018**, 34, 15622.

[28] a) K. Kuribayashi, S. Takeuchi, in *2008 IEEE 21st International Conference on Micro Electro Mechanical Systems*, DOI: 10.1109/memsys.2008.4443651, 2008, 296; b) S. Kresák, T. Hianik, R. L. C. Naumann, *Soft Matter* **2009**, 5, 4021; c) R. Ronen, Y. Kaufman, V. Freger, *J. Membr. Sci.* **2017**, 523, 247.

[29] a) H. Suzuki, K. Tabata, Y. Kato-Yamada, H. Noji, S. Takeuchi, *Lab Chip* **2004**, 4, 502; b) W. Wang, L. Monlezun, M. Picard, P. Benas, O. Francais, I. Broutin, B. Le Pioufle, *Analyst* **2012**, 137, 847; c) R. Kawano, T. Osaki, H. Sasaki, S. Takeuchi, *Small* **2010**, 6, 2100; d) M. E. Sandison, M. Zagnoni, H. Morgan, *Langmuir* **2007**, 23, 8277; e) F. Tomoike, T. Tonooka, T. Osaki, S. Takeuchi, *Lab Chip* **2016**, 16, 2423.

[30] N. Malmstadt, M. A. Nash, R. F. Purnell, J. J. Schmidt, *Nano Lett.* **2006**, 6, 1961.

[31] a) C. E. Stanley, K. S. Elvira, X. Z. Niu, A. D. Gee, O. Ces, J. B. Edel, A. J. Demello, *Chem. Commun. (Cambridge, U. K.)* **2010**, 46, 1620; b) Y. Elani, X. C. Solvas, J. B. Edel, R. V. Law, O. Ces, *Chem. Commun. (Cambridge, U. K.)* **2016**, 52, 5961.

[32] a) M. E. Dugger, C. A. Baker, *Anal. Bioanal. Chem.* **2019**, 411, 4605; b) M. Kitta, H. Tanaka, T. Kawai, *Biosens. Bioelectron.* **2009**, 25, 931; c) F. Tomoike, T. Tonooka, T. Osaki, S. Takeuchi, in *2015 28th IEEE International Conference on Micro Electro Mechanical Systems (MEMS)*, DOI: 10.1109/memsys.2015.7050931, 2015, 235.

[33] P. C. Hu, S. Li, N. Malmstadt, *ACS Appl. Mater. Interfaces* **2011**, 3, 1434.

[34] M. Le Berre, A. Yamada, L. Reck, Y. Chen, D. Baigl, *Langmuir* **2008**, 24, 2643.

[35] N. D. Kalyankar, M. K. Sharma, S. V. Vaidya, D. Calhoun, C. Maldarelli, A. Couzis, L. Gilchrist, *Langmuir* **2006**, 22, 5403.

[36] D. Stamou, C. Duschl, E. Delamarche, H. Vogel, *Angew. Chem. Int. Ed.* **2003**, 42, 5580.

[37] M. R. Horton, C. Reich, A. P. Gast, J. O. Radler, B. Nickel, *Langmuir* **2007**, 23, 6263.

[38] S. Matosevic, B. M. Paegel, *J. Am. Chem. Soc.* **2011**, 133, 2798.

[39] K. Karamdad, R. V. Law, J. M. Seddon, N. J. Brooks, O. Ces, *Lab Chip* **2015**, 15, 557.

[40] L. Lu, J. W. Schertzer, P. R. Chiarot, in *13th International Conference on Nanochannels, Microchannels, and Minichannels*, DOI: 10.1115/ICNMM2015-48556, California, U.S.A. 2015, 1.
[41] S. Y. Teh, R. Khnouf, H. Fan, A. P. Lee, *Biomicrofluidics* **2011**, 5, 44113.
[42] S. Maktabi, J. W. Schertzer, P. R. Chiarot, *Soft Matter* **2019**, 15, 3938.
[43] P. J. Chien, Y. L. Shih, C. T. Cheng, H. L. Tu, *Lab Chip* **2022**, 22, 2540.
[44] N. N. Deng, M. Yelleswarapu, L. Zheng, W. T. Huck, *J. Am. Chem. Soc.* **2017**, 139, 587.
[45] S. Deshpande, Y. Caspi, A. E. Meijering, C. Dekker, *Nat. Commun.* **2016**, 7, 10447.
[46] A. Jahn, W. N. Vreeland, M. Gaitan, L. E. Locascio, *J. Am. Chem. Soc.* **2004**, 126, 2674.
[47] T. A. Balbino, N. T. Aoki, A. A. M. Gasperini, C. L. P. Oliveira, A. R. Azzoni, L. P. Cavalcanti, L. G. de la Torre, *Chem. Eng. J.* **2013**, 226, 423.
[48] R. R. Hood, D. L. DeVoe, *Small* **2015**, 11, 5790.
[49] J. C. Stachowiak, D. L. Richmond, T. H. Li, A. P. Liu, S. H. Parekh, D. A. Fletcher, *Proc. Natl. Acad. Sci. U. S. A.* **2008**, 105, 4697.
[50] K. Kamiya, T. Osaki, S. Takeuchi, *Sens. Actuators, B* **2021**, 327, 128917.
[51] M. Gotanda, K. Kamiya, T. Osaki, N. Miki, S. Takeuchi, *Sens. Actuators, B* **2019**, 292, 57.
[52] K. Kuribayashi, G. Tresset, P. Coquet, H. Fujita, S. Takeuchi, *Meas. Sci. Technol.* **2006**, 17, 3121.
[53] K. S. Phillips, Q. Cheng, *Anal. Chem.* **2005**, 77, 327.
[54] A. Ainla, I. Gözen, B. Hakonen, A. Jesorka, *Sci. Rep.* **2013**, 3, 2743.
[55] L. Kam, S. G. Boxer, *J. Am. Chem. Soc.* **2000**, 122, 12901.
[56] S. Majd, M. Mayer, *Angew. Chem. Int. Ed.* **2005**, 44, 6697.
[57] A. R. Ferhan, B. K. Yoon, S. Park, T. N. Sut, H. Chin, J. H. Park, J. A. Jackman, N. Cho, *Nat. Protoc.* **2019**, 14, 2091.
[58] H. Su, H.-Y. Liu, A.-M. Pappa, T. C. Hidalgo, P. Cavassin, S. Inal, R. M. Owens, S. Daniel, *ACS Appl. Mater. Interfaces* **2019**, 11, 43799.
[59] P. Jönsson, M. P. Jonsson, F. Höök, *Nano Lett.* **2010**, 10, 1900.
[60] H. Suzuki, K. V. Tabata, H. Noji, S. Takeuchi, *Langmuir* **2006**, 22, 1937.
[61] T. Osaki, Y. Watanabe, R. Kawano, H. Sasaki, S. Takeuchi, *J. Microelectromech. Syst.* **2011**, 20, 797.
[62] M. Ł. Górzny, N. L. Opara, V. A. Guzenko, V. J. Cadarso, H. Schift, X. D. Li, C. Padeste, *Micro Nano Eng.* **2019**, 3, 31.
[63] O. Sadao, T. Wei-Heong, S. Hiroaki, T. Shoji, presented at 2008 IEEE 21st International Conference on Micro Electro Mechanical Systems, 13-17 Jan. 2008, **2008**.
[64] K. Shoji, R. Kawano, *Micromachines* **2018**, 9, 253.
[65] I. Hutter, E. Müller, P. M. Kristiansen, S. Kresak, L. Tiefenauer, *Microfluid. Nanofluid.* **2012**, 14, 421.
[66] P. J. Beltramo, R. Van Hooghten, J. Vermant, *Soft Matter* **2016**, 12, 4324.
[67] P. Heo, S. Ramakrishnan, J. Coleman, J. E. Rothman, J. B. Fleury, F. Pincet, *Small* **2019**, 15, e1900725.
[68] Y. Tsuji, R. Kawano, T. Osaki, K. Kamiya, N. Miki, S. Takeuchi, *Lab Chip* **2013**, 13, 1476.
[69] M.-A. Nguyen, S. A. Sarles, in *Conference on Smart Materials, Adaptive Structures and Intelligent Systems*, DOI: 10.1115/smasis2016-9034, VT, U.S.A. 2016, 1.
[70] M. Gotanda, K. Kamiya, T. Osaki, S. Fujii, N. Misawa, N. Miki, S. Takeuchi, presented at 2018 40th Annual International Conference of the IEEE Engineering in Medicine and Biology Society (EMBC), 18-21 July 2018, **2018**.

[71] S. Fujiwara, K. Shoji, C. Watanabe, R. Kawano, M. Yanagisawa, *Micromachines* **2020**, 11, 701.
[72] M. A. Czekalska, T. S. Kaminski, K. Makuch, P. Garstecki, *Sens. Actuators, B* **2019**, 286, 258.
[73] C. Reich, M. B. Hochrein, B. Krause, B. Nickel, *Rev. Sci. Instrum.* **2005**, 76, 095103.
[74] N. N. Deng, M. Yelleswarapu, W. T. Huck, *J. Am. Chem. Soc.* **2016**, 138, 7584.
[75] a) A. S. Utada, E. Lorenceau, D. R. Link, P. D. Kaplan, H. A. Stone, D. A. Weitz, *Science* **2005**, 308, 537; b) L. Y. Chu, A. S. Utada, R. K. Shah, J. W. Kim, D. A. Weitz, *Angew. Chem. Int. Ed.* **2007**, 46, 8970.
[76] M. Michelon, D. R. B. Oliveira, G. de Figueiredo Furtado, L. Gaziola de la Torre, R. L. Cunha, *Colloids Surf., B* **2017**, 156, 349.
[77] D. Carugo, J. Y. Lee, A. Pora, R. J. Browning, L. Capretto, C. Nastruzzi, E. Stride, *Biomed. Microdevices* **2016**, 18, 4.
[78] J. C. Stachowiak, D. L. Richmond, T. H. Li, F. Brochard-Wyart, D. A. Fletcher, *Lab Chip* **2009**, 9, 2003.
[79] K. Funakoshi, H. Suzuki, S. Takeuchi, *J. Am. Chem. Soc.* **2007**, 129, 12608.
[80] S. R. Kirchner, A. Ohlinger, T. Pfeiffer, A. S. Urban, F. D. Stefani, A. Deak, A. A. Lutich, J. Feldmann, *J. Biophotonics* **2012**, 5, 40.
[81] a) P. Lenz, C. M. Ajo-Franklin, S. G. Boxer, *Langmuir* **2004**, 20, 11092; b) J. T. Elliott, D. L. Burden, J. T. Woodward, A. Sehgal, J. F. Douglas, *Langmuir* **2003**, 19, 2275.
[82] P. Jonsson, J. P. Beech, J. O. Tegenfeldt, F. Hook, *J. Am. Chem. Soc.* **2009**, 131, 5294.
[83] S. R. Tabaei, J. A. Jackman, M. Kim, S. Yorulmaz, S. Vafaei, N. J. Cho, *J. Visualized Exp.* **2015**, DOI: 10.3791/5307353073.
[84] T. Maekawa, H. Chin, T. Nyu, T. N. Sut, A. R. Ferhan, T. Hayashi, N. J. Cho, *Phys. Chem. Chem. Phys.* **2019**, 21, 16686.
[85] a) S. R. Tabaei, S. Vafaei, N. J. Cho, *Phys. Chem. Chem. Phys.* **2015**, 17, 11546; b) H. Xu, H. Tae, N. J. Cho, C. Huang, K. J. Hsia, *Micromachines* **2022**, 13, 134; c) H. Tae, C. Yang, N.-J. Cho, *Acc. Mater. Res.* **2022**, 3, 1272; d) S. R. Tabaei, J. H. Choi, G. Haw Zan, V. P. Zhdanov, N. J. Cho, *Langmuir* **2014**, 30, 10363; e) S. R. Tabaei, J. A. Jackman, S. O. Kim, B. Liedberg, W. Knoll, A. N. Parikh, N. J. Cho, *Langmuir* **2014**, 30, 13345; f) S. Neupane, K. Betlem, F. U. Renner, P. Losada-Pérez, *Phys. Status Solidi A* **2021**, 218, 2000662.
[86] E. T. Castellana, P. S. Cremer, *Surf. Sci. Rep.* **2006**, 61, 429.
[87] A. Kumar, H. A. Biebuyck, G. M. Whitesides, *Langmuir* **1994**, 10, 1498.
[88] P. Mueller, D. O. Rudin, H. T. Tien, W. C. Wescott, *Nature* **1962**, 194, 979.
[89] S. Demarche, K. Sugihara, T. Zambelli, L. Tiefenauer, J. Voros, *Analyst* **2011**, 136, 1077.
[90] a) B. Liu, D. Rieck, B. J. Van Wie, G. J. Cheng, D. F. Moffett, D. A. Kidwell, *Biosens. Bioelectron.* **2009**, 24, 1843; b) J. A. Maurer, V. E. White, D. A. Dougherty, J. L. Nadeau, *Biosens. Bioelectron.* **2007**, 22, 2577.
[91] N. Fertig, C. Meyer, R. H. Blick, C. Trautmann, J. C. Behrends, *Phys. Rev. E* **2001**, 64, 40901.
[92] M. C. Peterman, J. M. Ziebarth, O. Braha, H. Bayley, H. A. Fishman, D. M. Bloom, *Biomed. Microdevices* **2002**, 4, 231.
[93] M. Mayer, J. K. Kriebel, M. T. Tosteson, G. M. Whitesides, *Biophys. J.* **2003**, 85, 2684.
[94] a) B. Le Pioufle, H. Suzuki, K. V. Tabata, H. Noji, S. Takeuchi, *Anal. Chem.* **2008**, 80, 328; b) M. Zagnoni, M. E. Sandison, P. Marius, H. Morgan, *Anal. Bioanal. Chem.* **2009**, 393, 1601.

[95] K. G. Klemic, J. F. Klemic, M. A. Reed, F. J. Sigworth, *Biosens. Bioelectron.* **2002**, 17, 597.
[96] Y. Huang, G. G. Fuller, V. Chandran Suja, *Adv. Colloid Interface Sci.* **2022**, 304, 102666.
[97] K. Funakoshi, H. Suzuki, S. Takeuchi, *Anal. Chem.* **2006**, 78, 8169.
[98] G. Ohlsson, S. R. Tabaei, J. Beech, J. Kvassman, U. Johanson, P. Kjellbom, J. O. Tegenfeldt, F. Hook, *Lab Chip* **2012**, 12, 4635.
[99] S. Li, P. C. Hu, N. Malmstadt, *Biophys. J.* **2011**, 101, 700.
[100] S. Li, P. Hu, N. Malmstadt, *Anal. Chem.* **2010**, 82, 7766.
[101] P. Kuhn, K. Eyer, S. Allner, D. Lombardi, P. S. Dittrich, *Anal. Chem.* **2011**, 83, 8877.
[102] M. Schaich, J. Cama, K. Al Nahas, D. Sobota, H. Sleath, K. Jahnke, S. Deshpande, C. Dekker, U. F. Keyser, *Mol. Pharmaceutics* **2019**, 16, 2494.
[103] J. Kaur, H. Ghorbanpoor, Y. Ozturk, O. Kaygusuz, H. Avci, C. Darcan, L. Trabzon, F. D. Guzel, *IET Nanobiotechnol.* **2021**, 15, 100.
[104] T. Bhatia, T. Robinson, R. Dimova, *Soft Matter* **2020**, 16, 7359.
[105] L. Chao, S. Daniel, *J. Am. Chem. Soc.* **2011**, 133, 15635.
[106] T. Nisisako, S. A. Portonovo, J. J. Schmidt, *Analyst* **2013**, 138, 6793.
[107] E. B. Stephenson, K. S. Elvira, *Chem. Commun. (Cambridge, U. K.)* **2021**, 57, 6534.
[108] S. Bachler, M. Ort, S. D. Kramer, P. S. Dittrich, *Anal. Chem.* **2021**, 93, 5137.
[109] C. L. Kuyper, J. S. Kuo, S. A. Mutch, D. T. Chiu, *J. Am. Chem. Soc.* **2006**, 128, 3233.
[110] J. P. Monteiro, A. F. Martins, M. Lucio, S. Reis, T. J. Pinheiro, C. F. Geraldes, P. J. Oliveira, A. S. Jurado, *Toxicol. In Vitro* **2011**, 25, 1215.
[111] C. Provin, A. Nicolas, S. Grégoire, T. Fujii, *Pharm. Res.* **2015**, DOI: 10.1007/s11095-015-1654-x2704.
[112] J. Cama, C. Chimerel, S. Pagliara, A. Javer, U. F. Keyser, *Lab Chip* **2014**, 14, 2303.
[113] S. Majd, D. J. Estes, M. Mayer, *Calcium Bind Proteins* **2006**, 1, 26.
[114] H. Mao, T. Yang, P. S. Cremer, *J. Am. Chem. Soc.* **2002**, 124, 4432.
[115] T. Robinson, P. S. Dittrich, *ChemBioChem* **2019**, 20, 2666.
[116] S. Puza, S. Asfia, R. Seemann, J. B. Fleury, *Int. J. Mol. Sci.* **2023**, 24, 2072.

Author biographies



Eduarda Fernandes is pursuing a PhD in Materials Engineering at Centre of Physics from universities of Minho and Porto (Portugal), and BCMaterials (Spain). Throughout her early scientific carrier, she has been acquiring expertise on the application of biophysical techniques to decipher the molecular phenomena of the interactions between drugs/bioactives and lipid biomimetic models. Recently, she has been focusing on the Material Science field, where she is acquiring expertise towards the development on innovative lipid microfluidic-based *in vitro* high-throughput screening tools for pharmaceutical and cosmetics industries.



Vanessa F. Cardoso received the M.Sc. degree in biomedical engineering with specialization in medical electronics in 2008, and the PhD. degree in 2012, all from the University of Minho-UM, Portugal. Since 2021, she is an Assistant Researcher at the Microelectromechanical Systems Research Unit-CMEMS from UM. Her research work has been focused design and fabrication of microfluidic platforms for biomedical applications. She has been also working actively on the development, processing, characterization, and validation of smart and (multi)functional materials with tailored physicochemical properties for various (bio)technological applications and on the development of green chemistry approaches.



Senentxu Lanceros-Méndez is Ikerbasque Professor at BCMaterials, Basque Center for Materials, Applications and Nanostructures, Leioa, Spain, where he is the Scientific Director. He is Associate Professor at the Physics Department of the University of Minho, Portugal (on leave), where also belongs to the Center of Physics of the Univesity of Minho and Porto. He graduated in Physics at the University of the Basque Country, Leioa, Spain and obtained his PhD at the Institute of Physics of the Julius-Maximilians-Universität Würzburg, Germany. His work is focused on the development of smart and multifunctional materials for sensors and actuators, energy, environmental and biomedical applications.



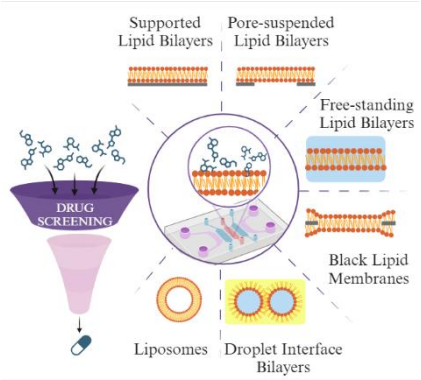
Marlene Lúcio is PharmD by Faculty of Pharmacy of University of Porto, and PhD in Pharmaceutical Chemistry by the same institution. Since 2014 is an Assistant Researcher/Invited Professor from Centre of Molecular and Environmental Biology (CBMA) and Centre of Physics of the University of Minho and Porto (CF-UM-UP). Her research is focused on two aims: (i) using biomimetic and *in silico* models with high throughput/greener processes for refining the design of nanotherapeutics, with less animal experimentation and lower reagent and effluent consumption (ii) developing multifunctional nanosystems to tackle major concerning diseases or to repurpose classical low effective drugs.

Table of contents

Effective drug discovery and molecular optimization procedures depend heavily on a comprehensive understanding of the reciprocal drug-membrane interactions. This review explores recent developments in microfluidic lipid biomimetic models for screening these interactions. A synopsis of lipid-based drug screening models is provided, along with a deeper analysis of the most promising microfluidic methods for their production and applications on drug screening.

Eduarda Fernandes, Vanessa F. Cardoso, Senentxu Lanceros-Méndez and Marlene Lúcio

Lipid Microfluidic Biomimetic Models for Drug Screening: a comprehensive review


Supported
Lipid Bilayers
Pore-suspended
Lipid Bilayers
Free-standing
Lipid Bilayers
DRUG
SCREENING
Black Lipid
Membranes
Liposomes
Droplet Interface
Bilayers